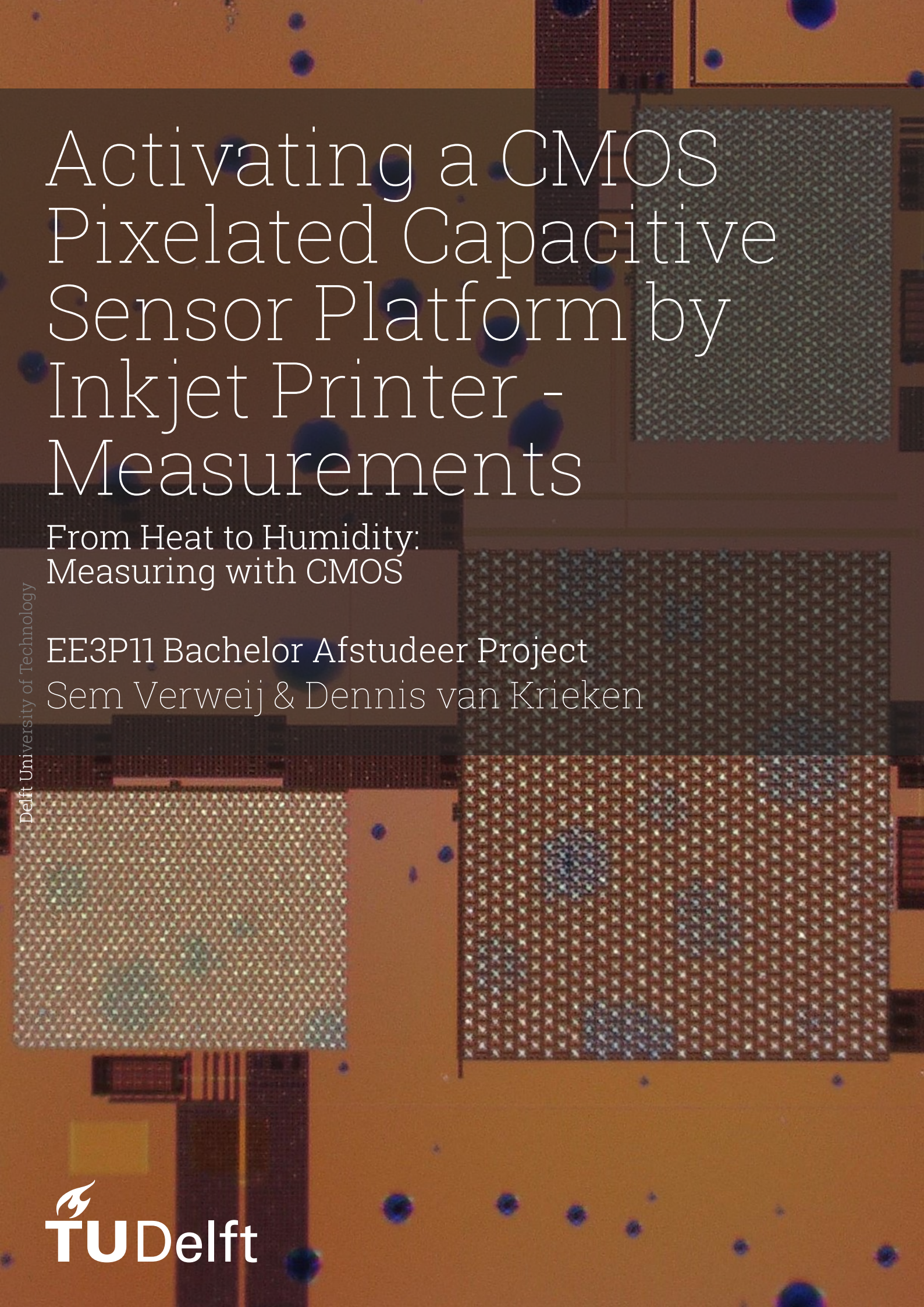

Activating a CMOS Pixelated Capacitive Sensor Platform by Inkjet Printer - Measurements

From Heat to Humidity: Measuring with CMOS

EE3P11 Bachelor Afstudeer Project

Sem Verweij & Dennis van Krieken

Delft University of Technology

TU Delft

Activating a CMOS Pixelated Capacitive Sensor Platform by Inkjet Printer - Measurements

From Heat to Humidity: Measuring with CMOS

by

Sem Verweij & Dennis van Krieken

In collaboration with

N. Chen
T.A. Tommel
D. Rueda Lindemann
E. Tuinstra

Student Name	Student Number
Sem Verweij	5610435
Dennis van Krieken	5475317

Supervisors:	dr. S. Kundu & prof.dr.ir. F. P. Widdershoven
Daily Supervisor:	T. Shen
Project Duration:	April, 2024 - June, 2024
Faculty:	Faculty of Electrical Engineering, Mathematics & Computer Science, Delft

Cover: A Close-up of an inked chip

TU Delft

Preface

As this project comes to an end, it marks the end of a three-year-long journey towards a Bachelor's Degree in Electrical Engineering. This project has allowed us to explore the world of sensors, and in particular CMOS sensors.

We are deeply grateful for the guidance and support from our two supervisors, Prof.dr.ir F.P. Widdershoven and dr. S. Kundu as well as our daily supervisor T. Shen without whom this project would have never been possible. Additionally, we would like to express our gratitude to Delft University of Technology and NXP, who's resources were invaluable and essential to this project.

Throughout this project, three subgroups have worked together to bring this project to fruition. Our primary contribution to the project is analysing the behaviour of the chip, shining light on its potential. And being the final step in a proof of concept that material can be printed on chips using a simple desktop printer.

We would like to highlight our deepest gratitude to our supervisor, dr. Suman Kundu, for his unparalleled guidance and being ever present during the entire project. Without him, we would never have made the progress that has been made, he helped us find solutions or at least *"Think about it"*.

Sem Verweij & Dennis van Krieken
Delft, July 2024

Abstract

The Epson ET-8500 inkjet printer was modified to deposit precise quantities of ink on CMOS chips, enabling the fabrication of capacitive sensors. This project explores the potential of using affordable, consumer-grade printing technology for advanced sensor development, typically requiring expensive equipment. The research focused on understanding the interaction between printed ink and environmental variables such as humidity, light, and temperature. Three measurement setups were developed to detect capacitance changes under varying conditions. The setups for light and humidity successfully generated usable data, while the temperature setup needs redesigning for consistency. Key findings include the exponential relationship between humidity and capacitance in water-based inks. Light exposure generally decreased capacitance, except for white, zinc oxide and tin oxide under UV light. A machine learning model, using a neural network with a cross-entropy loss function, effectively identified inked electrodes but requires more variance in the datasets.

Contents

Preface i

Summary ii

1 Introduction 1
- 1.1 Inkjet Printers . . . 1
- 1.2 State of the Art . . . 1
- 1.3 Similar Research . . . 2
- 1.4 Synopsis . . . 2
- 1.5 Thesis Outline . . . 2

2 Project Overview 3
- 2.1 Problem Definition . . . 3
- 2.2 Program of Requirements . . . 4

3 Background Information 5
- 3.1 Introduction . . . 5
- 3.2 Chip . . . 5
- 3.3 Inks . . . 7
- 3.4 Principles behind dielectric changes . . . 9
  - 3.4.1 Humidity . . . 9
  - 3.4.2 Light . . . 9

4 Methods & Design Choices 10
- 4.1 Introduction . . . 10
- 4.2 Working Method . . . 10
- 4.3 Measurement Setups . . . 11
  - 4.3.1 Humidity . . . 11
  - 4.3.2 Light . . . 12
- 4.4 Adapter . . . 13
- 4.5 GUI . . . 14
  - 4.5.1 Visualizer . . . 14
  - 4.5.2 Averages over time . . . 15
  - 4.5.3 Bar Plotter . . . 16
  - 4.5.4 Machine Learning . . . 17

5 Results 19
- 5.1 Measurement Results . . . 19
  - 5.1.1 Light Measurements . . . 21
  - 5.1.2 365nm . . . 24
  - 5.1.3 Humidity Measurements . . . 25
- 5.2 Printed chips . . . 28
  - 5.2.1 Grid with same sized dots . . . 28
  - 5.2.2 Grid with different sized dots. . . . 29
  - 5.2.3 Multicoloured chip . . . 30

5.2.4 Various Thickness . . . 31
5.2.5 Various Colours . . . 32

6 Machine Learning **34**
6.1 Introduction . . . 34
6.2 Model Design . . . 34
6.3 Data Acquisition and Feature Extraction . . . 34
6.4 Results . . . 35

7 Discussion **37**
7.1 Discussion of the Machine Learning Model . . . 37
7.2 Future Recommendations . . . 38

8 Conclusions, recommendation and future work **40**

References **42**

A Tables **44**
A.1 Light Measurements . . . 44
A.1.1 Cyan . . . 44
A.1.2 Magenta . . . 44
A.1.3 Yellow . . . 45
A.1.4 Grey . . . 45
A.1.5 Black . . . 45
A.1.6 Photo Black . . . 46
A.1.7 White Ink . . . 46
A.1.8 Empty . . . 46
A.2 Moisture Measurements . . . 47
A.2.1 Cyan . . . 47
A.2.2 Magenta . . . 47
A.2.3 Yellow . . . 47
A.2.4 Grey . . . 48
A.2.5 Black . . . 48
A.2.6 Photo Black . . . 48
A.2.7 White Ink . . . 49
A.2.8 Empty . . . 49

B Temperature Measurements **50**
B.0.1 Temperature . . . 50
B.1 Measurement Setup . . . 50
B.2 Results . . . 51
B.3 Problem with the measurements setup . . . 52

C Derivations & compositions **53**
C.1 Switched Capacitor . . . 53
C.2 Ink Composition . . . 54
C.2.1 Magenta . . . 54
C.2.2 Cyan . . . 54
C.2.3 Yellow . . . 54

D Machine Learning Images **56**
D.1 Images of Ink Predictions . . . 56

1 Introduction

1.1 Inkjet Printers

Nowadays printing technology has become widespread, available to most if not all middle-class families. Despite its rather low costs, the technology is already very mature and can print to a very precise degree. The printer used for research in this thesis, the Epson ET-8500, has shown from testing that it is capable of printing with an incredible accuracy of up to a tenth of a millimeter of distance between two different droplets with ink droplets with a diameter of around 80 micrometers.

With this accuracy a lot more can be achieved than just daily printing jobs such as high precision deposit of fluids. If one were to be able to print on CMOS chips, then it would enable both in theory and in practice the fabrication of capacitive sensors readily available for anyone to do at home. This would make sensor technology a lot more accessible as compared to before, for one needed very expensive and complicated machinery to produce them. This in turn makes the product also rather expensive.

1.2 State of the Art

The Epson ET-8500 is an inkjet printer that uses a piezoelectric printing technology. This technology is currently the most reliable in terms of drop consistency and speed. It uses piezo-driven inkjet printhead that is activated by a voltage waveform applied to a piezoelectric transducer. This in turn changes in shape when activated, generating a pressure pulse in the ink chamber, causing a droplet of the printing substance to drop[1].

Although the technology is readily available, the option for a consumer to easily print any substance on any substrate is far from accessible. This is due to a few different reasons. Two of them being the nature of the printers usually only allowing for (easy) printing on paper, thus the transition to other substrates requires significant alterations to the printer and the second is that printing software is not properly documented for the public to view and ultimately to understand.

Despite the fact that manipulating a printer to do what a consumer exactly wants is made quite difficult by the manufacturers, there have been more people who have tried to control their printer through unconventional ways. Such ways can mean both the making of significant hardware changes as well as the use of driver commands. More on this will be mentioned in section 1.3 Similar Research.

On the other hand, if one were to refer to more advanced printers, which are usually known as material printers. Though, these do cross over more in the territory of 3D printers. As mentioned before, these printers can be rather pricey, with prices starting in the ten-thousands going up to over a million euros, but they can also be rather large, smaller ones are about double the size of household printers while the larger material printers can be as large as a a medium sized room, which also depends on the kind of material that is printed by the printer.

Theoretically, these more expensive printers are also able to print on a resolution of up to 1200 dpi up to an accuracy of even 2900 dpi. According to the documentation of the Epson ET-8500, it should have a printing resolution of up to 5760 x 1440 dpi. Although, in practice, the highest practical resolution 720 x 720 dpi. Though, taking into account the sizing of the printed dots, this is plenty for the manufacturing of capacitive CMOS sensors.

1.3 Similar Research

As previously mentioned, this project is not entirely unique in its premise of taking more or full control of a household printer.[2] In some cases an effort was also made to print on surfaces of one's own choosing. Other research also proved that using a printer's CD printing feature is usable as a platform to jump start the development from.[3] [4] [5]

Research has been done to investigate the potential of CMOS Pixelated capacitive sensors, the chips used have the same concept with it being arrays of electrodes[6][7][8]. The main working principle is the same as the chips that are available during the project.

Besides this, Inkjet printing has been employed to print entire sensors[9] or deposit material on existing electrodes that allowed it to detect humidity.[10]

1.4 Synopsis

Using this information and personal research, the latter of which will be reported on in this document. The printer was eventually modified to allow for cleaning with cleaning solutions altering the tubing with custom tubing, valves and extra ink tanks to store the cleaning fluid in. Next to that, direct printing on the chip using a tray for the chip, based on the tray for CDs and DVDs, together with the in-built CD and DVD printing function of the printer.

1.5 Thesis Outline

The thesis is structured as follows: In chapter 2 a problem definition will be described, after which a program of requirements is made. In chapter 3 the main inner workings of the chip will be explained and some background information is shown. In chapter 4 designs and methods will be discussed. In chapter 5 the results are shown and analysed. In chapter 7 the results and analysis will be interpreted, the implications will be discussed, and possible future research directions will be discussed. Finally, in chapter 8 a conclusion will be made.

2

Project Overview

In the modern world, almost everything uses sensors. Sensors, react to the environment and detect various conditions like: Temperature, humidity, light and pressure. But also Heart rates, the presence of certain gasses and acceleration are determined using sensors. Sensors play a crucial part of our lives, they make our lives easier and their applications are endless. The goal of this project is to create an easy, safe inexpensive way of depositing sensor material on chips.

2.1 Problem Definition

For the Bap, the task was to modify a printer that is able to deposit picolitre amounts of ink accurately on a chip. The ET-8500 printer from Epson was used, which is a conventional, relatively inexpensive table-top printer. This printer was chosen because it is of the Ecotank line. Which allows us to fill the tanks with any fluid required. Furthermore, it possesses a CD-tray and poster printing capabilities, which would allow for enough vertical space for the packaged chips to fit.

The project is divided into three subgroups:

- Hardware
- Software
- Measurements

In Figure 2.1 the entire process of from chip to readout is visualized. Outlined by red is the part handled by the measurements group

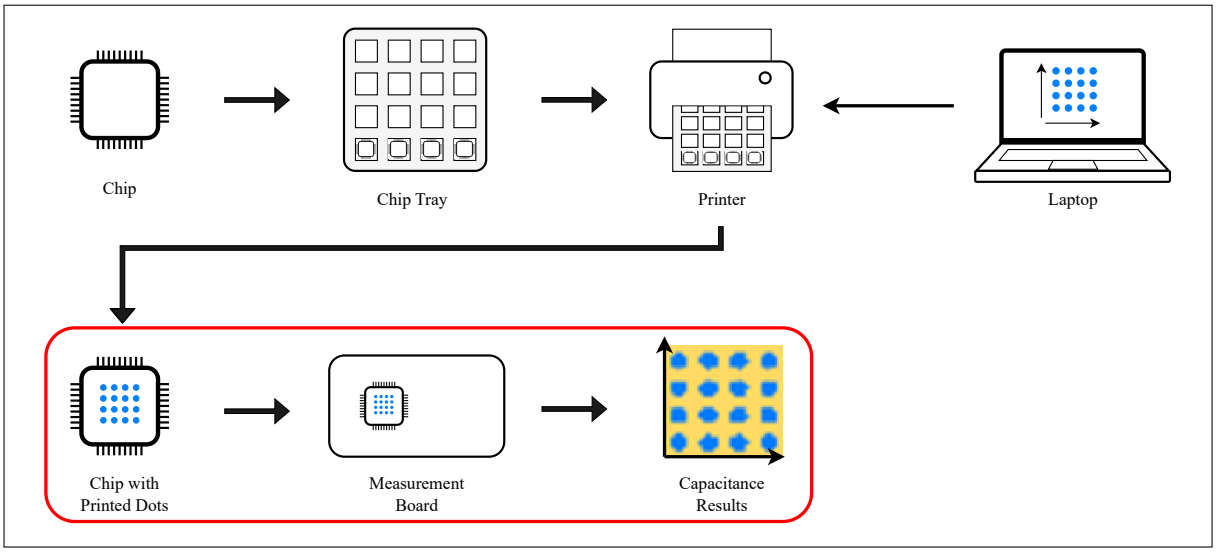

Figure 2.1: Project Diagram: Measurements Group

A general overview of tasks given to the Measurement Group. Is:

1. Running measurements with printed chips and interpreting acquired data from the functionalized CMOS-pixelated capacitive sensor array
2. How the printed ink signal varies with different light signals, different temperatures, and different relative humidity values, and different Volatile Organic Compounds
3. Distinguishing different colour inks via machine learning using their capacitance values.

These tasks result in the problem definition:

> *"Develop a comprehensive understanding of the interaction between printed ink signals and environmental variables, using a functionalized CMOS-pixelated capacitive sensor array. This includes the ability to distinguish inks using their capacitance values"*

2.2 Program of Requirements

From the tasks and problem definition a program of requirements is setup.

Measurements Setup

[1.1] Develop a measurement setup for different environmental conditions

[1.2] Collect and Interpret data from the functionalized CMOS-pixelated capacitive sensor array

[1.3] Design a QFP44 to DIP24 adapter to readout printed chips.

Characterization

[2.1] Asses the influence of different wavelengths of light on different inks.

[2.2] Asses the influence of various humidity levels on different inks.

[2.3] Asses the influence of various Temperature levels on different inks.

[2.4] Develop a meaningful Machine Learning classification model.

3

Background Information

3.1 Introduction

The chip used contains three sensor arrays with different layouts, each array has a different layout with different electrode sizes and different spacings between the electrodes, a close-up can be seen in Figure 3.1. For this project, the focus will be on the largest array.

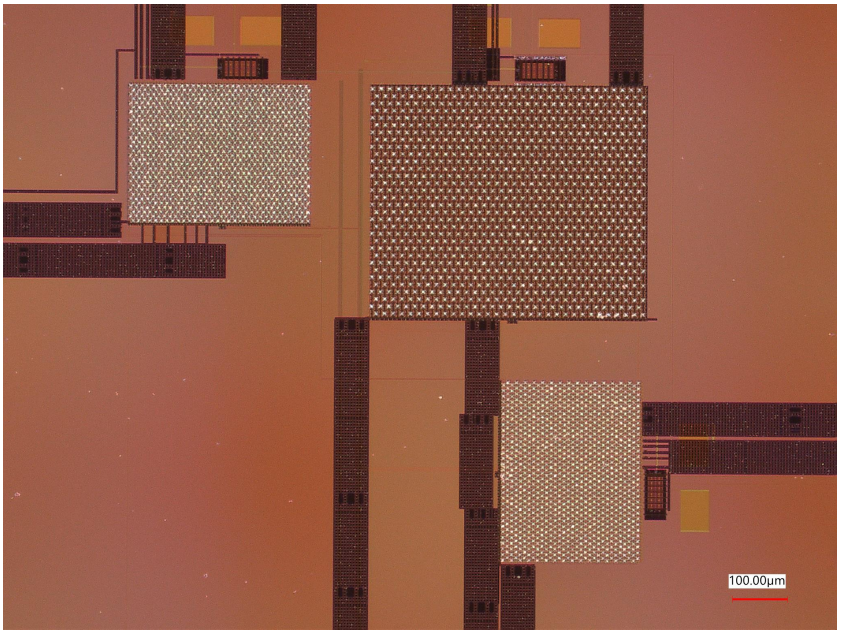

Figure 3.1: Close up view of a chip

3.2 Chip

The capacitance is generated by the electric fields between the electrode and all other electrodes around it. To measure this capacitance, two transistors work in tandem.

A piece of a single column is illustrated in Figure 3.2b. Let's say the objective is to measure the capacitance of C_0. A cycle is started, first $Q_{T,0}$ is set to high to open the transistor and let the electrode charge, then $Q_{T,0}$ goes low and $Q_{D,0}$ goes high to let the build up charge out. Every

cycle a charge dependent on the capacitance and parasitic capacitance is released to ground.

The average current that flows through the sensor electrodes is mirrored by a PMOS current mirror and amplified on a 1:10 ratio. The output current of this PMOS Mirror then flows into a NMOS current mirror where it is amplified 1:10 again. Therefore, the initial current is amplified 1:100 times. This amplification factor is determined by the physical properties of the Mosfets namely their with/length ratio. A PMOS Mirror can be found in Figure 3.2a

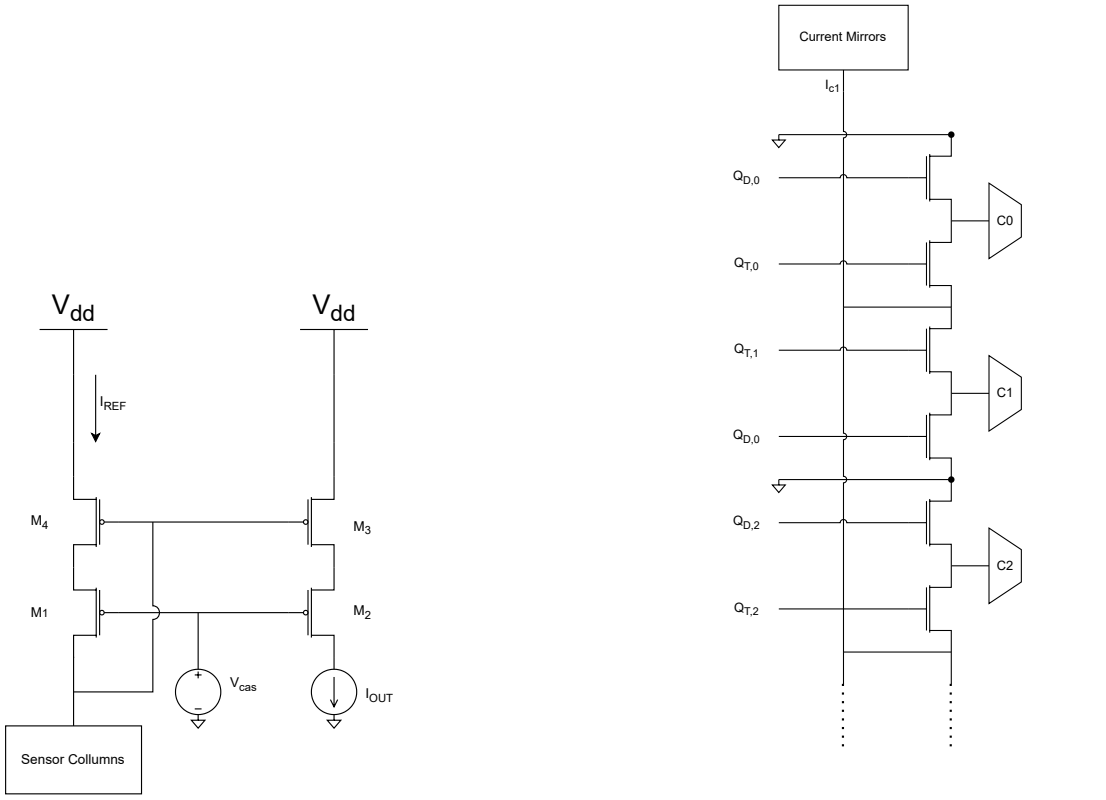

(a) Pmos Current Mirror

(b) Piece of collumn from sensor array

Figure 3.2: IC Chip Design, a P-type current mirror(left) and a piece of the sensor array (right)

This current goes through a transimpedance amplifier stage on the measurements board where the output current is amplified further and converted to an output voltage. This voltage can be determined as

$$V = V_{bias} + 100 I_C \cdot 68k\Omega \tag{3.1}$$

Where

- V is the voltage at the output of the amplifier (V),
- V_{bias} is the bias voltage of the amplifier (V),
- I_C is the current through the sensor column (A),

this then gets converted by an ADC according to the relationship found in Equation 3.2.

$$\lfloor ADC \rceil = \frac{V_{in}}{3.3V} 4096 \tag{3.2}$$

Where

- ADC is the read-out ADC value.

By changing the dielectric medium between the electrodes, the permittivity changes and so does the resulting current.

The two switched and electrode needed to read out together form a switched capacitor. Of which the current can be described using the following relationship:

$$I_C = CV_{dd}f \tag{3.3}$$

where

- C is the capacitance of the electrode (F),
- V is the voltage between V_{dd} and ground,
- f is the frequency in (Hz),

The derivation of this equation can be found in section C.1. V_{dd} can be altered using the measurements board and is set to 1.1 V during this project. Combining Equation 3.1, Equation 3.2 & Equation 3.3 results in.

$$\lfloor ADC \rceil = \frac{V_{bias} + 100CV_{dd}f \cdot 68k\Omega}{3.3V} 4096 \tag{3.4}$$

3.3 Inks

The inks used can be found in Table 3.1 & Table 3.2 & Table 3.3 where a dash represents unknown/unmentioned.

Table 3.1: Chemical composition of various printer inks from Material Safety Data Sheet documents

Component	Black	Cyan	Magenta	Yellow
Water	65-80%	65-80%	65-80%	65-80%
Glycerol	5-7%	10-12.5%	10-12.5%	7-10%
TEGBE	3-5%	7-10%	7-10%	7-10%
Tetramethyldecynediol	0.25-0.5%	0.1-0.25%	0.1-0.25%	0.25-0.5%
Triethanolamine	0.5-1%	0.1-0.25%	0.1-0.25%	0.1-0.25%
Benzisothiazolinone	-	0.0015%-0.05%	0.0015%-0.05%	0.0015%-0.05%
Carbon black	5-7%	-	-	-

Table 3.2: Chemical composition of various printer inks from Material Safety Data Sheet documents

Component	Grey	Photo Black
Water	65-80%	65-80%
Glycerol	7-10%	7-10%
TEGBE	7-10%	7-10%
Tetramethyldecynediol	0.1-0.25%	-
Triethanolamine	-	0.1-0.25%
Benzisothiazolinone	0.0015-0.05%	0.0015-0.05%
Carbon black	-	-
E-BK105	-	1-3%

Table 3.3: Chemical composition of white printer ink from Material Safety Data Sheet documents

Component	White
1-ethoxy-2-(2-methoxyethoxy)ethane	65-80%
Titanium Dioxide	12.5-15%
(2-Methoxymethylethoxy)propanol	5-7%
Gamma-Butyrolactone	1-3%

Where

- Water: main solvent
- Glycerol: improves flow properties and helps control viscosity
- TEGBE[1]: functions as solvent
- Tetramethyldecynediol[2]: functions as a defoamer.
- Triethanoamine: functions as an emulsifier
- Benzisothiazolinone[3]: functions as a preservative.
- Carbon Black: functions as main colourant of the black coloured ink.
- E-BK105: functions as main colourant in photo black ink.
- 1-ethoxy-2-(2-methoxyethoxy)ethane: main solvent
- Titanium Dioxide: functions as main colourant in white ink.

As can be seen from Table 3.1, Table 3.2 and Table 3.3 for the majority of inks, the colourant is not shown. Only for Photo Black, normal black and white ink the colourant is known. Typically, cyan contains copper phthalocyanine its chemical formula can be found in Figure C.2, grey is a mixture of black colourant and another colourant dependent on the desired hues, magenta is a salt of which the chemical composition can be found in Figure C.1 and yellow is a combination of various salts which can be found in Figure C.3. All inks are water based, except for the white ink. The white ink is 1-ethoxy-2-(2-methoxyethoxy)ethane based.

[1]Triethylene Glycol Monobutyl Ether
[2]2,4,7,9-tetramethyldec-5-yne-4,7-diol
[3]1,2-benzisothiazolin-3- one

3.4 Principles behind dielectric changes

Humidity

When the relative humidity increases, more water is adsorbed onto the ink. For each relative humidity percentage, a sorption isotherm indicates the corresponding water content at a constant temperature. This sorption isotherm behaviour changes for different material properties.

If the ink is more porous and is able to contain more water content, the dielectric constant changes as air is replaced by water. And since

$$C = C_0 \epsilon_r \tag{3.5}$$

Where

1. C is the capacitance with
2. ϵ_r is the relative static permittivity
3. C_0 is the capacitance with vacuum dielectric

the change in capacitance is linear to the change in dielectric.

Sorption isotherms with different porosity have different classifications. These classifications range from S curves to exponential relations[11][12]. These isotherms are related to the type of material. For example, one of the main components of the inks after drying is glycerol, glycerol is hydrophilic and when the relative humidity increases, the water content in glycerol can be represented by an exponential curve[13]. The main colourant in black is Carbon Black, Carbon Black has a porous structure and is not soluble. Therefore, when there is high humidity capillary condensation takes place where the water vapour adsorbs into these pores, these pores fill until maximum hydration after which saturation takes place, the resulting isotherm would be an S type curve.

Light

If light with a wavelength of the emission/absorption spectrum is shined on the inks, it is possible that electrons are excited to a higher energy state and change its polarization properties. This can increase the material's dielectric constant and therefore its capacitance. From Equation 3.3 and Equation 3.5 we can see that an increase in dielectric results in a larger current and thus a larger ADC value is read.

4

Methods & Design Choices

4.1 Introduction

In this chapter, any designs made will be discussed. Besides the designs, measurement setups will be shown and their respective methodology will be explained.

4.2 Working Method

Using a measurement board, it was possible to read the values from the chips. In preparation for the goal of printing onto the chips with the printer, ink was drop-cast onto eight existing chips: one chip for each of the seven colors of ink and one empty chip. For drop-casting, a 2 ml syringe was used. The syringe was filled with a small amount of ink and a relatively large volume of air. By applying a high pressure to the syringe, tiny drops of ink were ejected and landed on the chip array.

Using a measurement board, it was possible to read the values from the chips. These chips were measured under different environmental conditions and analysed. The conditions tested included: UV light, RGB light, temperature, and humidity. Which electrode is inked or uninked is determined by an image of the array, made by a high resolution microscope. An example of a readout and an image of the array can be seen in Figure 4.1. This readout figure was made using python.

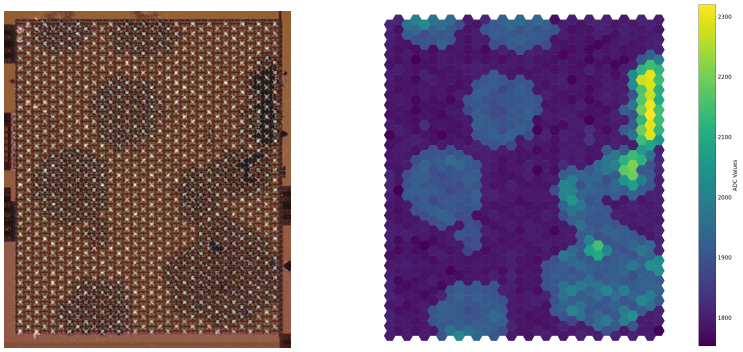

(a) Visual of inked chip **(b)** Readout

Figure 4.1: Visual of the chip and its ADC readout

4.3 Measurement Setups

The chips are tested on three different categories of environmental conditions: Humidity and Light and Temperature. Three measurement setups have been developed that each control an aspect of the environment. Unfortunately, the temperature measurement setup produced unreliable data and was therefore excluded from any further analysis. Details of the attempt to control the temperature are provided in Appendix B.

Humidity

A humidity chamber was constructed to enable precise control of relative humidity.

The humidity level inside the chamber can be increased by pouring water through a straw located on the side of the chamber. The water lands on a sponge, spreads out, and subsequently evaporates, raising the humidity level.

To decrease the humidity level, the air inside the chamber can be replaced with pure dry nitrogen gas, which contains no moisture. Consequently, introducing nitrogen gas reduces the humidity inside the chamber. A gas hose connector is positioned at the back of the chamber for connection to a nitrogen gas tank. It is important to note that nitrogen gas contains no oxygen and poses a risk of suffocation.

The chamber is sealed with a lid secured by pressure from two side handles. Additional foam has been added around the brim to ensure a tight seal. A hole was drilled in the side of the chamber to accommodate the chip. The hole matches the size of the ZIF socket precisely. This ensures that the chip is situated within the humidity chamber, while the micro-controller and cables remain outside. The humidity level and temperature within the chamber are monitored by a humidity sensor affixed to the side of the box adjacent to the chip. The humidity chamber effectively maintained a stable relative humidity range from 10% to 90% The humidity chamber can be observed in Figures 4.2

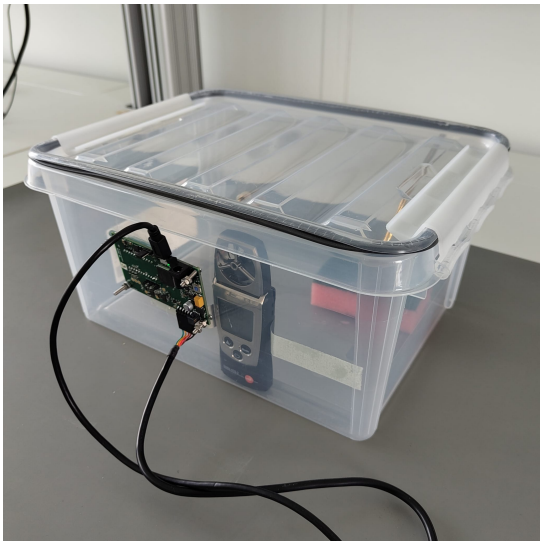

(a) Humidity chamber sealed

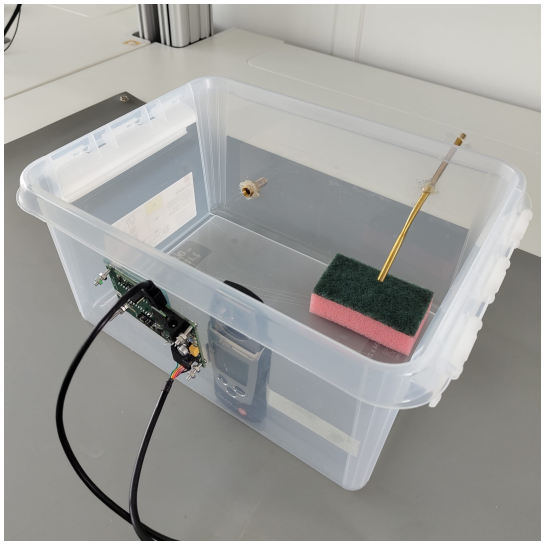

(b) Humidity chamber Open

Figure 4.2: The humidity chamber.

Light

To observe the behaviour of the chips under different light conditions, a set of flashlights, each emitting a different wavelength of light, was directed at the measurement board. Each flashlight was mounted on a stand using a clamp, positioned at a distance of 2.5 cm from the chip. The entire setup was placed inside a light exclusion box to block any external light sources.

A humidity and temperature sensor was employed to monitor the room's relative humidity and temperature. This is the same sensor utilised in the humidity setup. The light measurement setup is depicted in Figure 4.3.

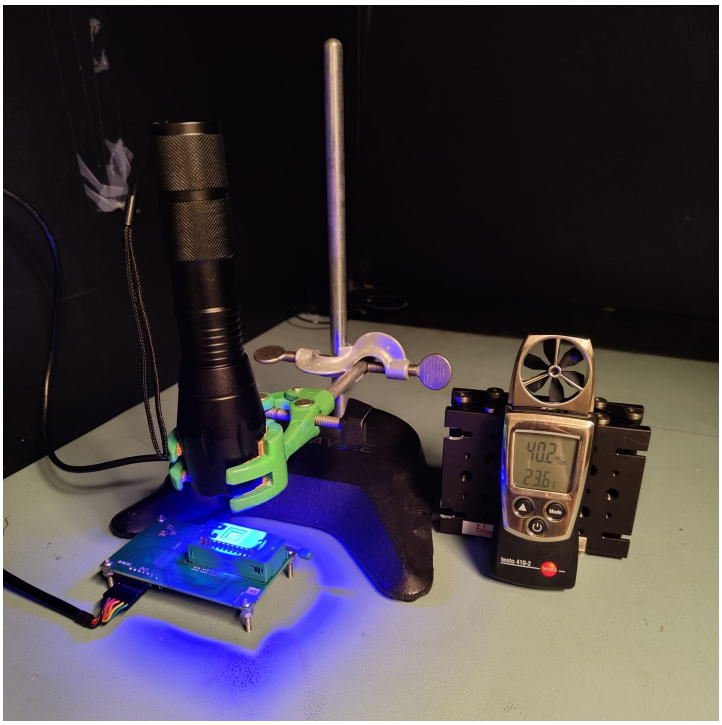

Figure 4.3: The light measurement setup.

4.4 Adapter

To connect to a chip a package was needed. Since open-top packages are only available in certain pin layouts, the decision was made for the LQFP44 package or the Low Quad Flat Package with 44 pins the connections can be found in Figure 4.4 with the outside numbers representing the DIP24 pin numbers and the inside numbers representing the QFP44 pin numbers. Unfortunately, the readout board has a ZIF with 24 slots, as that was what was originally required. So an adapter had to be designed, two designs were made. One design allowed the QFP44 package to be soldered to the PCB which would allow for permanent fixture for measurements. The other design included a Clamshell test and burn-in socket. Which would allow for quick and easy package swapping of the packages. The second design also required a second adapter board as the pins of the clamshell would not allow correctly spaced pin rows.

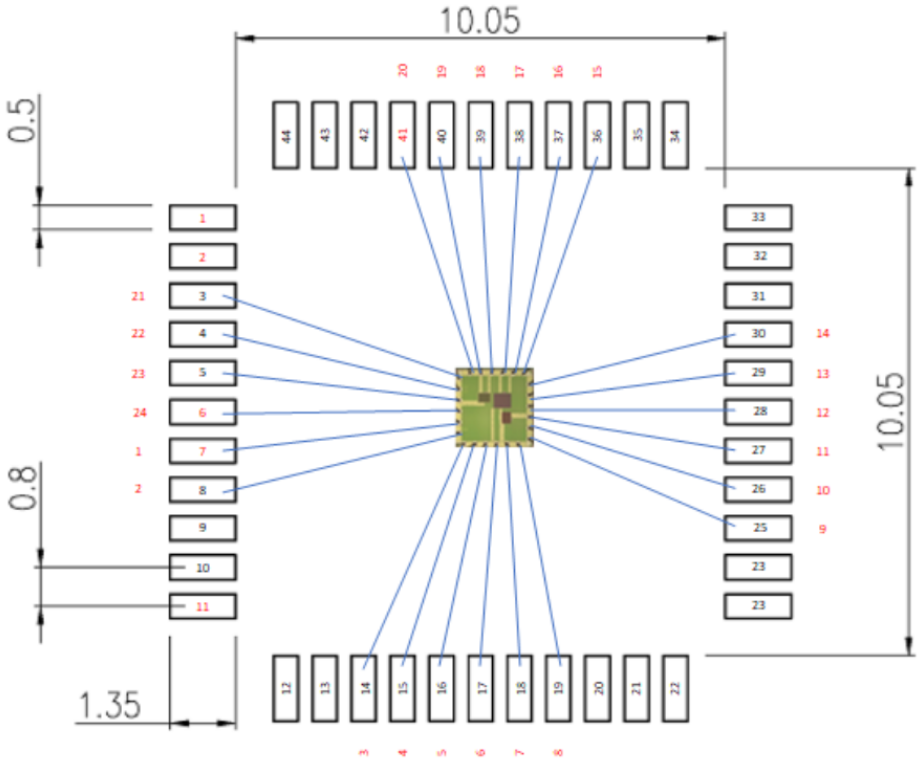

Figure 4.4: pin layout QFP44 to DIP24

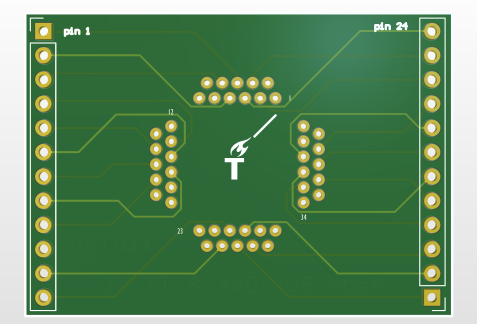

(a) Clamshell PCB Front

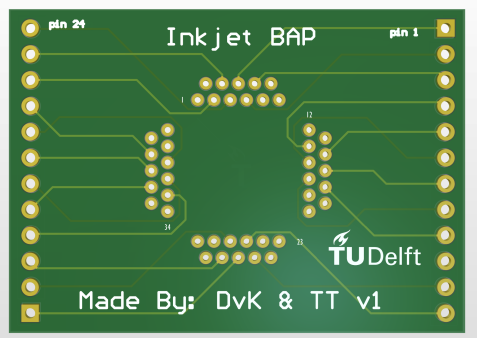

(b) Clamshell PCB Backside

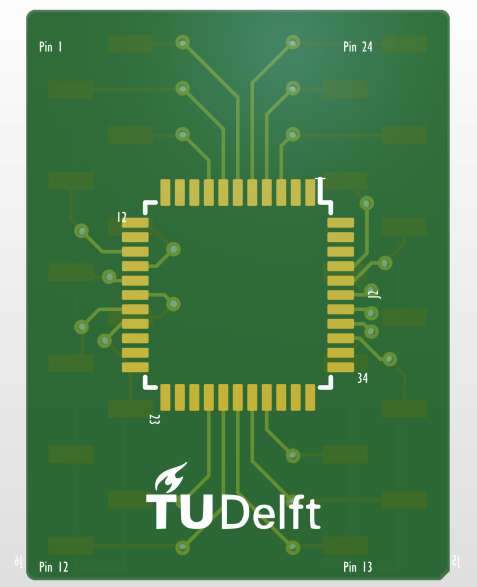

(c) Soldered PCB Front

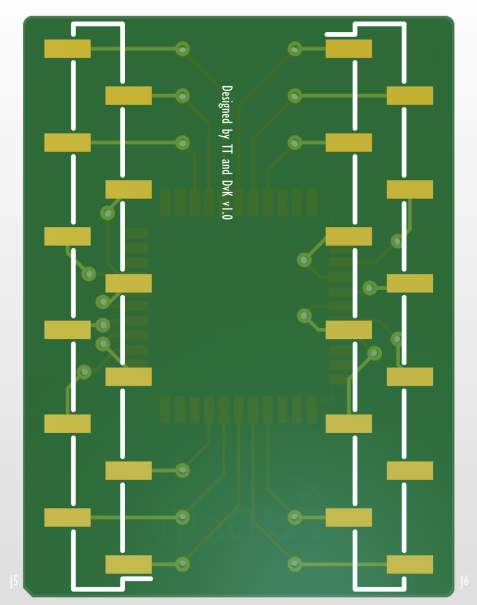

(d) Soldered PCB Backside

Figure 4.5: PCB Designs

4.5 GUI

For visualisation and analysis a GUI was developed. Figure 4.1b was made using this UI.

Visualizer

The first tab is made to visualize the data. Figure 4.6 shows the first tab. In this tab:

- The dropdown menu allows the user to switch between dark and light theme layout.
- Select File: allows the user to select a .dat file to display.
- The dropdown menu allows the user to switch between the three arrays.
- The two input boxes sets the lower and upper limits of the colour bar with a refresh button to refresh the plot.
- The plot is clickable, which allows the user to select inked and reference spots, red represents inked and pink represents reference.
- Using the toggle mode button, the user can switch between selecting inked and reference spots.

- Clear selection removes both selected and reference spots.
- The K-means button applies a simple K-means algorithm to automatically try to find the inked spots.
- The click a hexagon textbox shows the value of a hexagon when clicked.
- The import/Export selected buttons allow the user to load and export the selection and reference spots.
- The slider allows the user to view specific measurements.

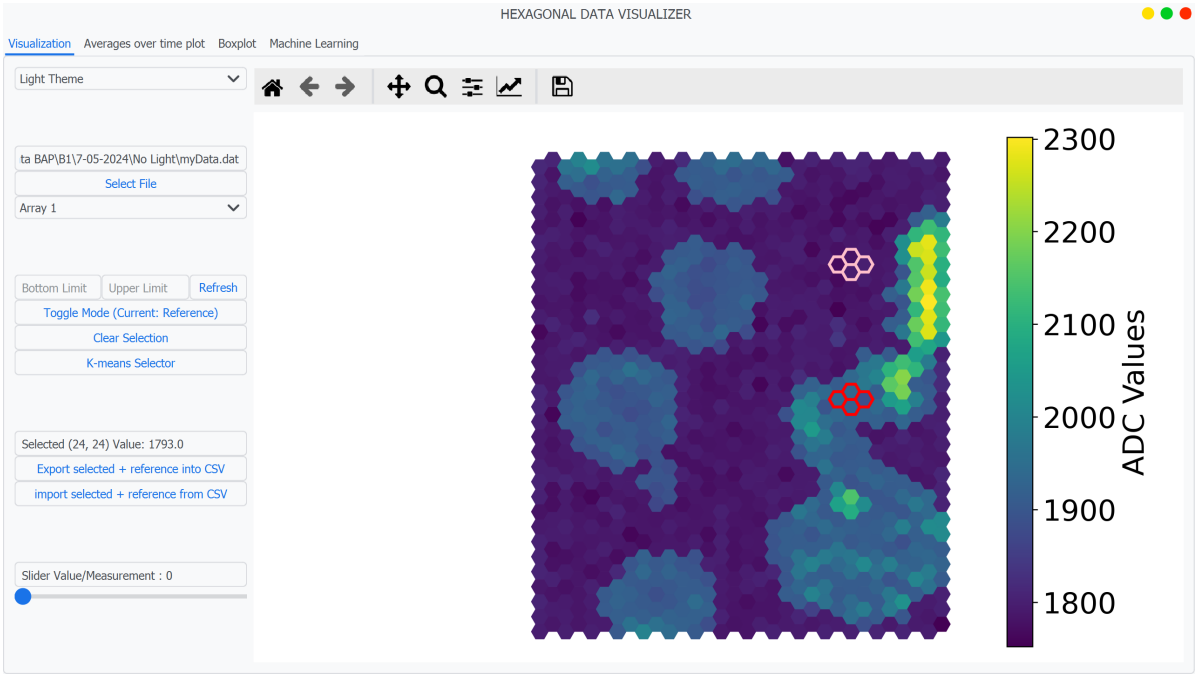

Figure 4.6: Visualizer

Averages over time

In this tab the user can plot the averaged selected and reference values selected from the previous slide through time. Figure 4.7 shows the second tab.

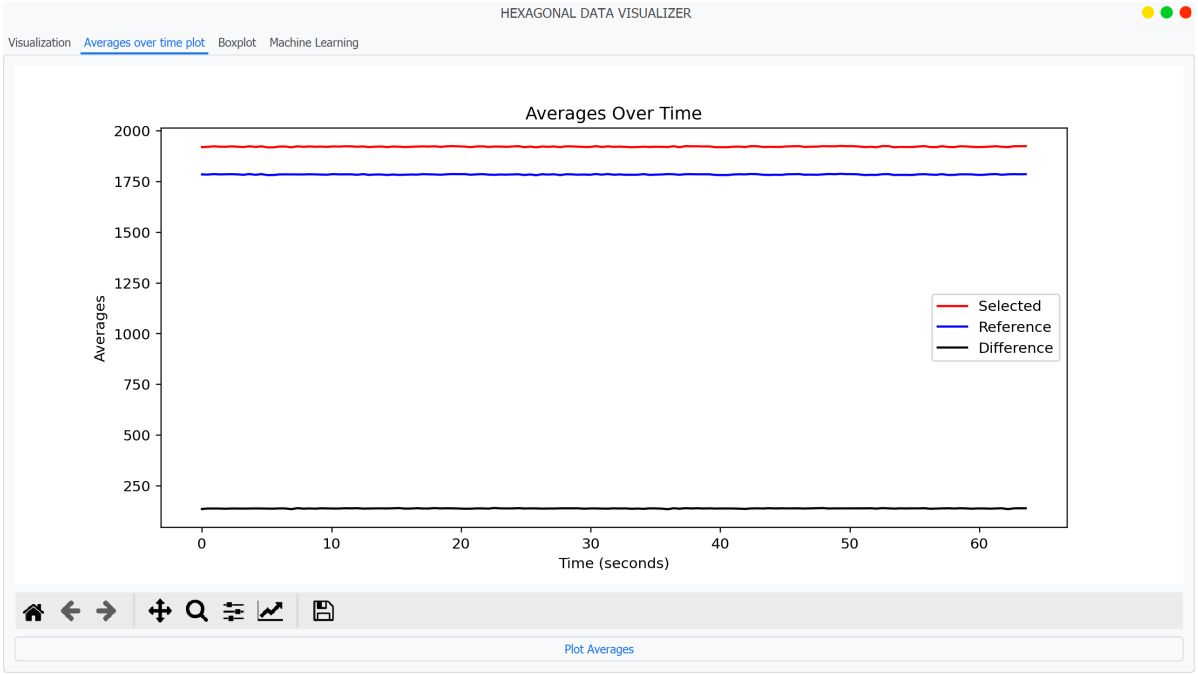

Figure 4.7: Values through time

Bar Plotter

In this tab, the user can plot their data. An example of plotted data through different humidities can be found in Figure 4.8. Here, the user can:

- Select their files using the select files button
- Select whether the signal and reference plots are desired or the difference between them needs to be plotted.
- The grid font size can be specified
- Select whether only the last 11 measurements should be used and reload the plot.
- A copy pastable Latex table for streamlined data visualisation.

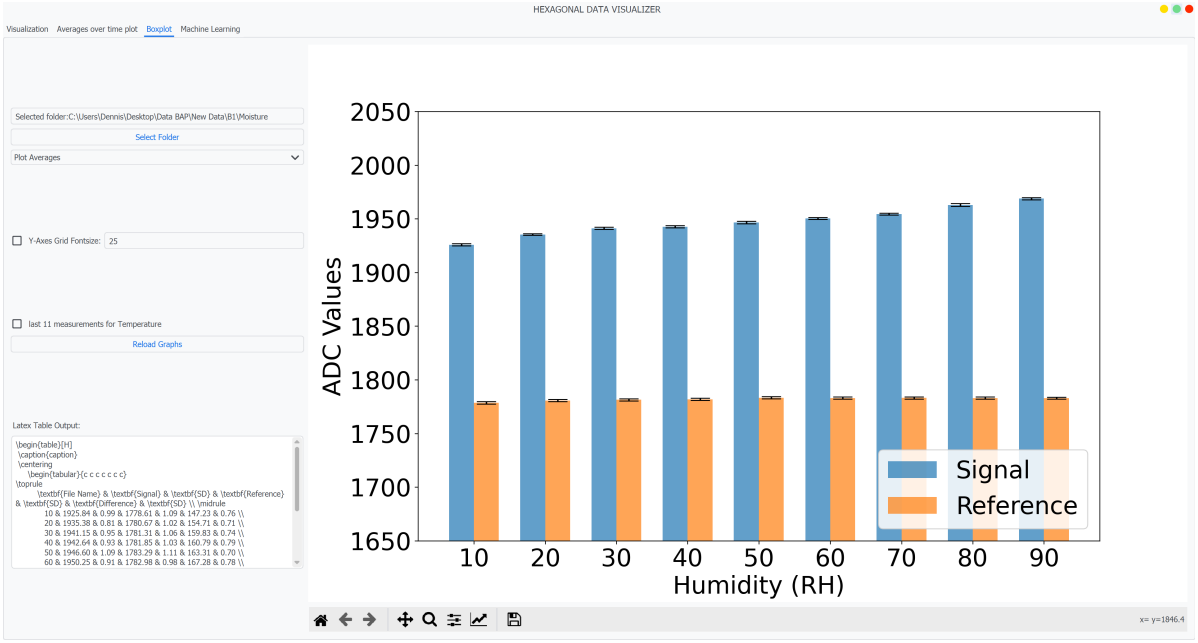

Figure 4.8: Bar Plots

Machine Learning

In this tab the user can predict what kind of inks are deposited. An example can be found in Figure 4.9. Here the user can:

- Select what chips are used in the training data
- Export the data
- Select what data is used for training
- Select which model is used.
- Select what test dataset is used.
- Test the model with the result being displayed on the right.

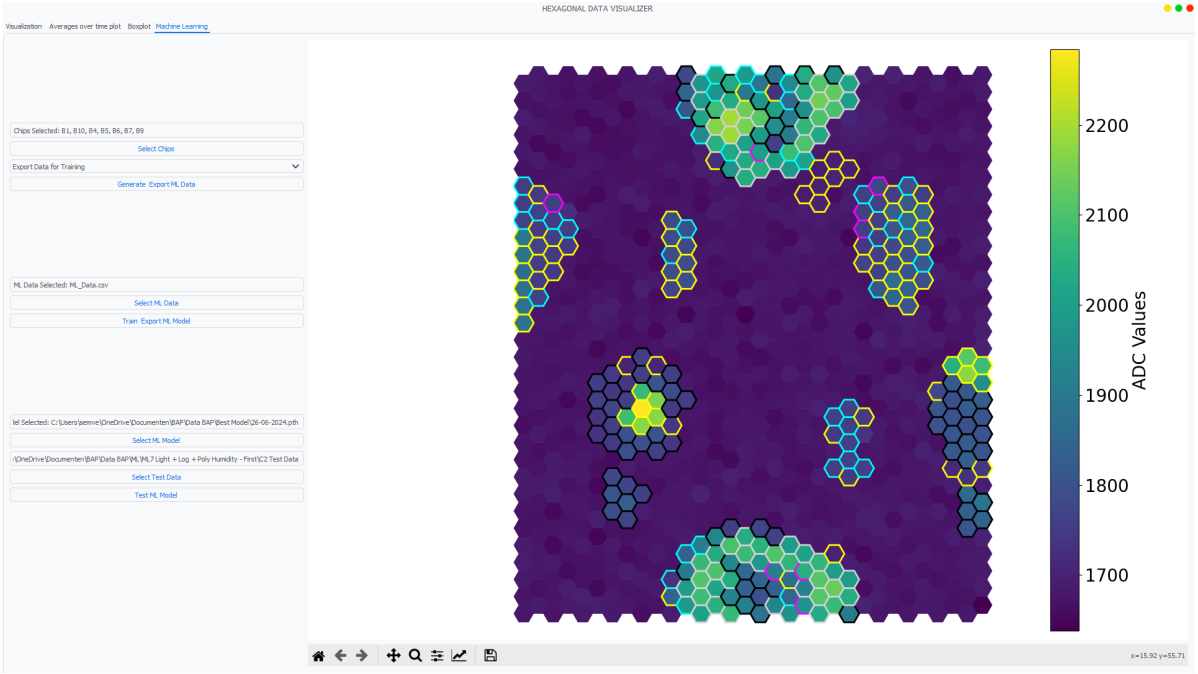

Figure 4.9: Machine Learning

5

Results

5.1 Measurement Results

The results from the humidity and light measurements are presented in Figures 5.2 to 5.18. In these graphs, the capacitance is presented as ADC values for each environmental condition. Data tables are provided in Appendix A.

The results include the mean signal from the inked electrodes, the mean values from the uninked electrodes, and the difference between these two sets of electrodes. In this report, the data from the uninked electrodes is referred to as the reference, and the data from the inked electrodes as the signal. The standard deviation of all three sets is included in the tables and shown in the graphs using a simplified boxplot, displaying only the upper and lower limits. The difference was determined by subtracting the mean of the reference data from the signal data.

No two chips are identical. The mean value of a chip is highly dependent on fabrication variations. This is illustrated in Figure 5.1, which displays the ADC values of multiple chips before any drop-casting or modification was performed. As shown, the mean values vary significantly. Calculating the difference can effectively mitigate the impact of these fabrication differences. Additionally, the difference helps mitigate noise experienced by both inked and uninked electrodes. Therefore, the differential data is the most reliable parameter to showcase the characteristic behaviour of the ink in different environments.

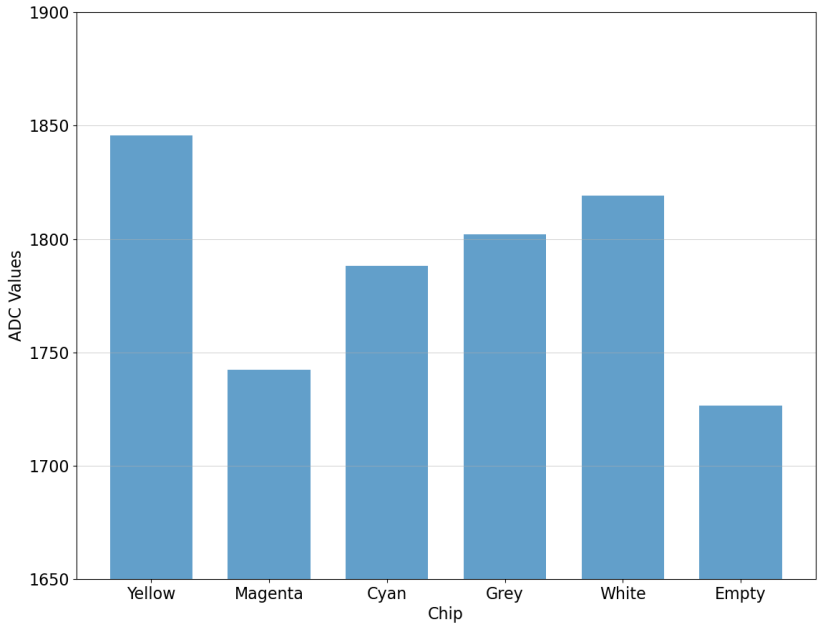

Figure 5.1: ADC values of the chips before the drop-casting of the corresponding color. Note: The measurement for the black chip is missing as it was never recorded, and the data for photo black is absent due to faulty data.

Light Measurements

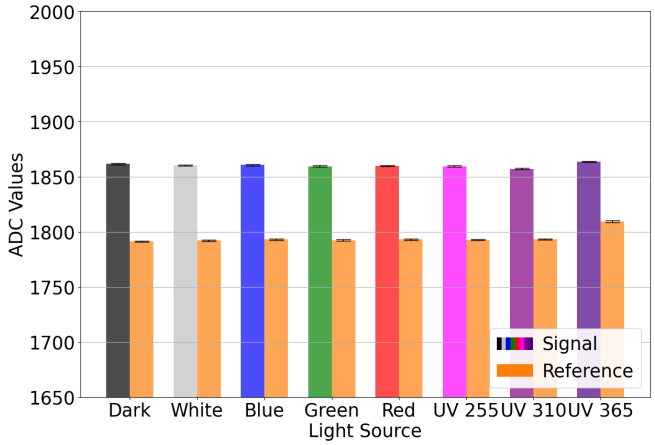

(a) Averages of signal and reference

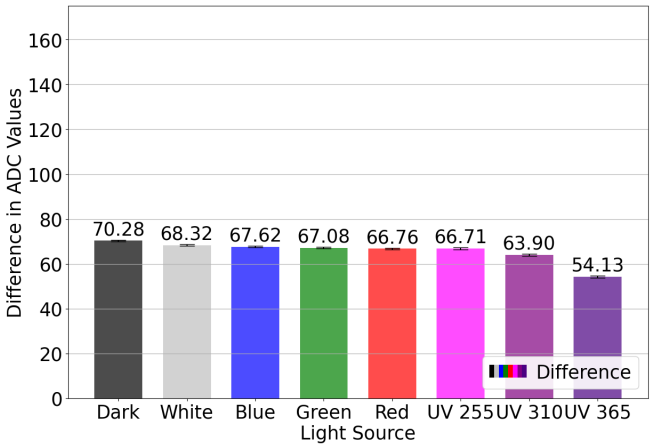

(b) Difference between signal and reference

Figure 5.2: Light measurements of a cyan inked chip.

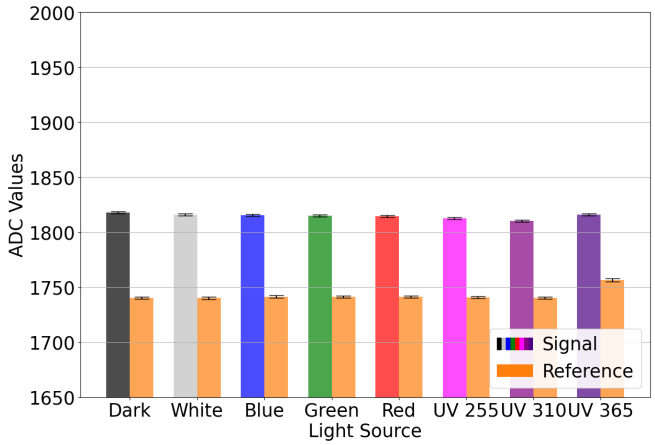

(a) Averages of signal and reference

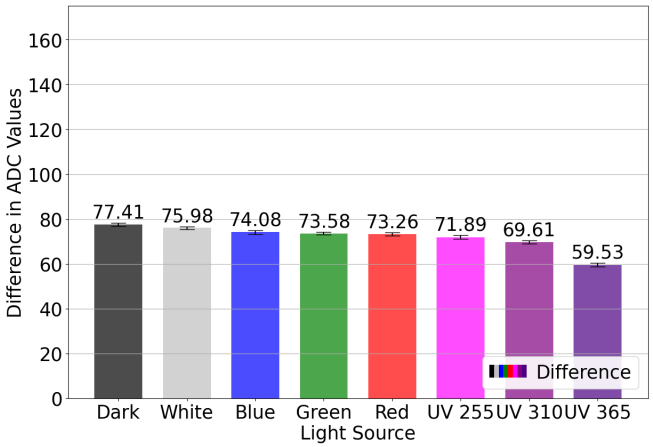

(b) Difference between signal and reference

Figure 5.3: Light measurements of a magenta inked chip.

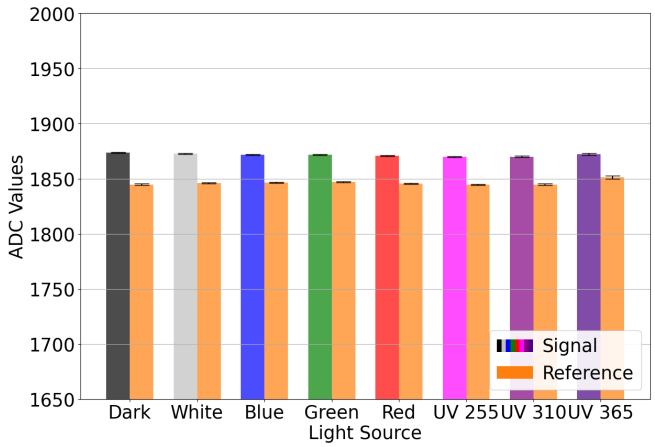

(a) Averages of signal and reference

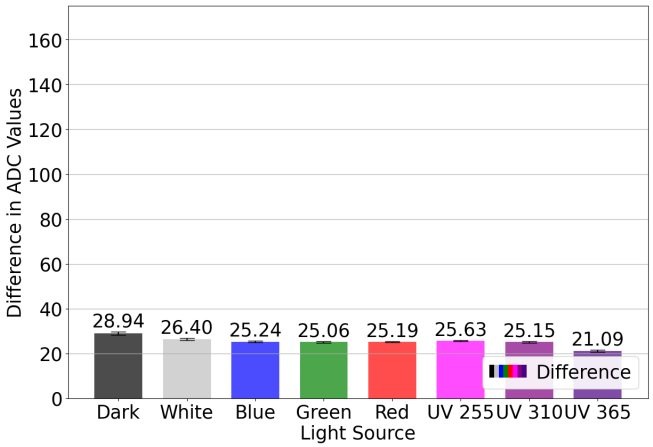

(b) Difference between signal and reference

Figure 5.4: Light measurements of a yellow inked chip.

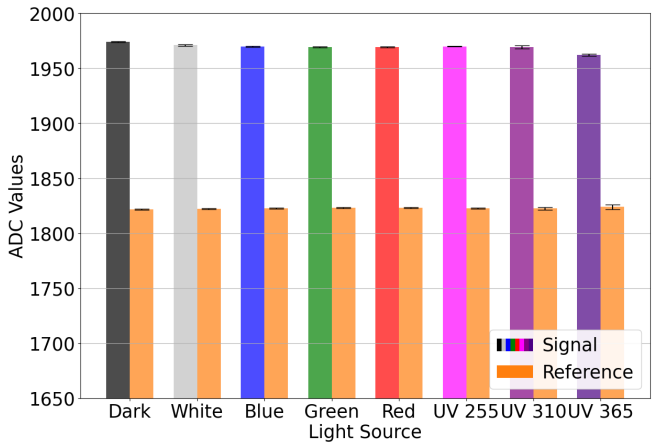

(a) Averages of signal and reference

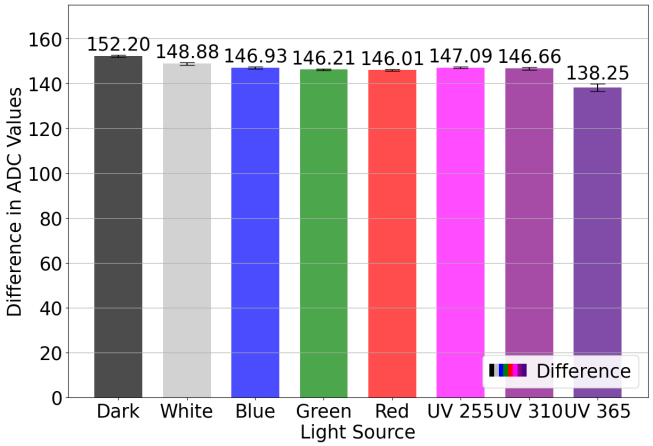

(b) Difference between signal and reference

Figure 5.5: Light measurements of a grey inked chip.

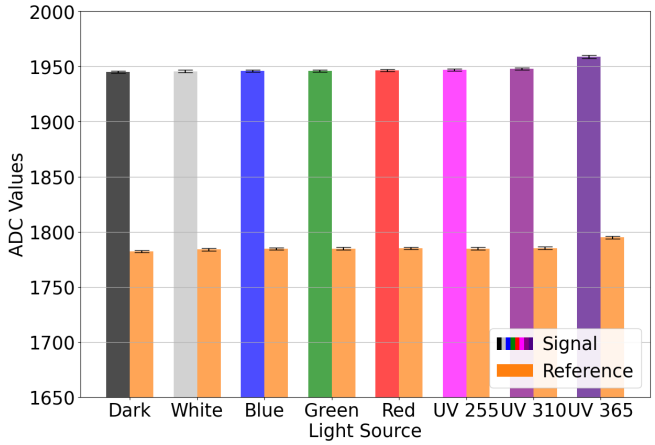

(a) Averages of signal and reference

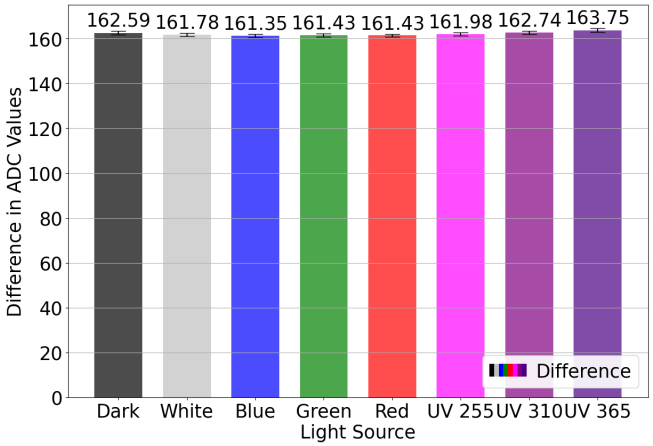

(b) Difference between signal and reference

Figure 5.6: Light measurements of a black inked chip.

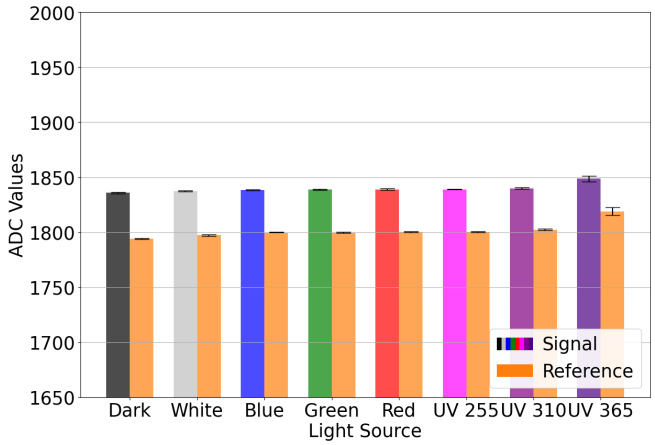

(a) Averages of signal and reference

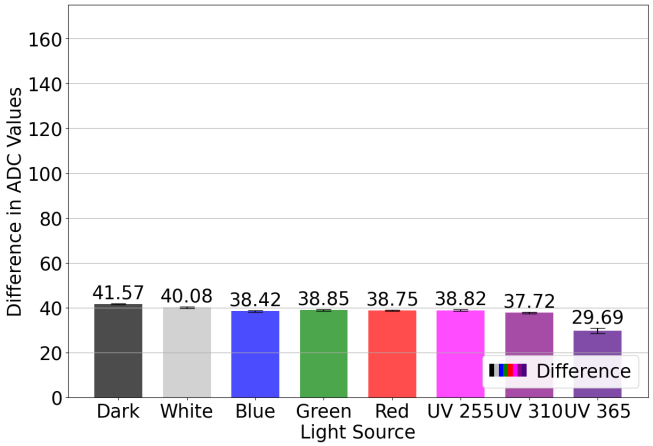

(b) Difference between signal and reference

Figure 5.7: Light measurements of a photo-black inked chip.

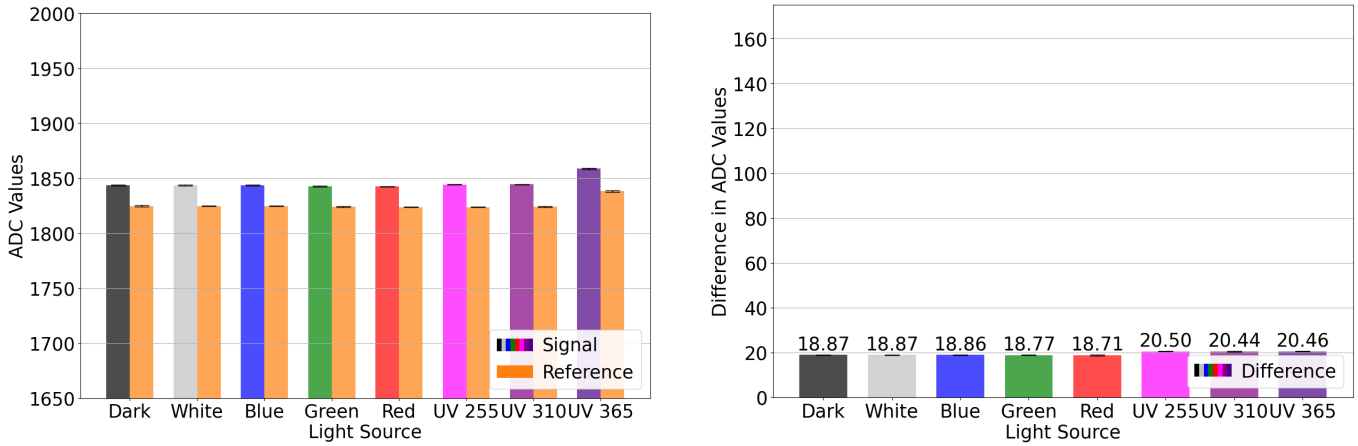

(a) Averages of signal and reference

(b) Difference between signal and reference

Figure 5.8: Light measurements of a white inked chip.

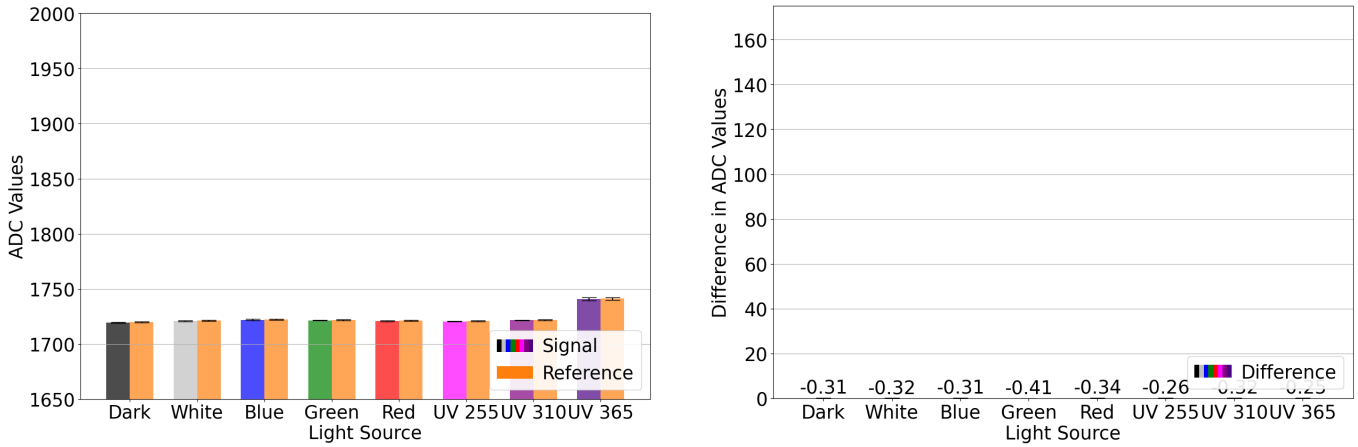

(a) Averages of signal and reference

(b) Difference between signal and reference

Figure 5.9: Light measurements of an empty chip.

365nm

As can be seen in the Figures the 365nm torch increases the values of the reference and for some the inked electrodes too. Shining the 365nm Torch on an empty chip gives a result which can be found in Figure 5.10. As we can see here there is a sharp increase after the torch is turned on and after its turned off it drops. This shows that the intense 365nm light from the torch influences the chip itself and not necessarily the ink.

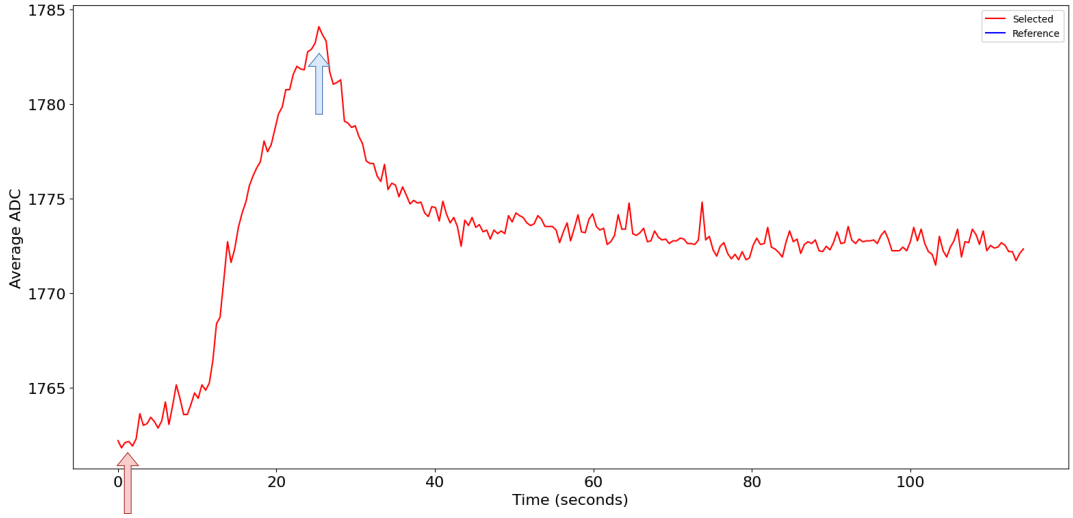

Figure 5.10: Empty chip with 365nm UV light shone upon it. the red arrow represents the light turned on, the blue arrow represents the light turned off.

Humidity Measurements

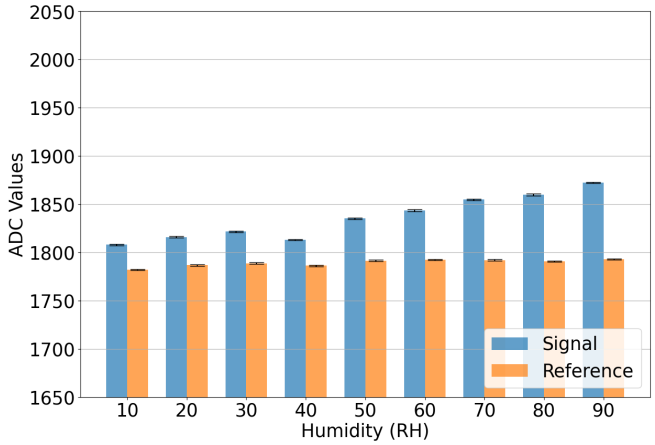

(a) Averages of signal and reference

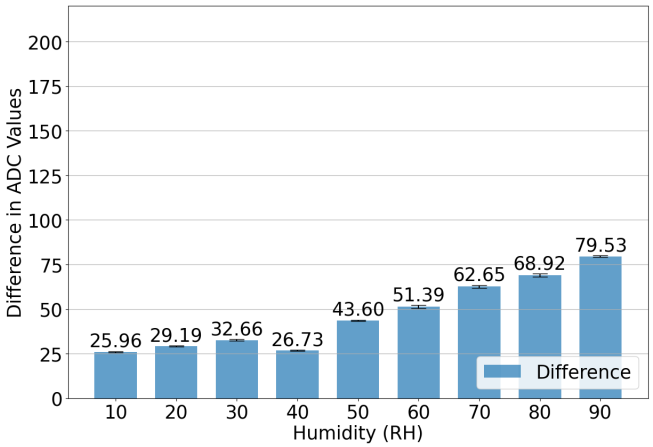

(b) Difference between signal and reference

Figure 5.11: Humidity measurements of a cyan inked chip.

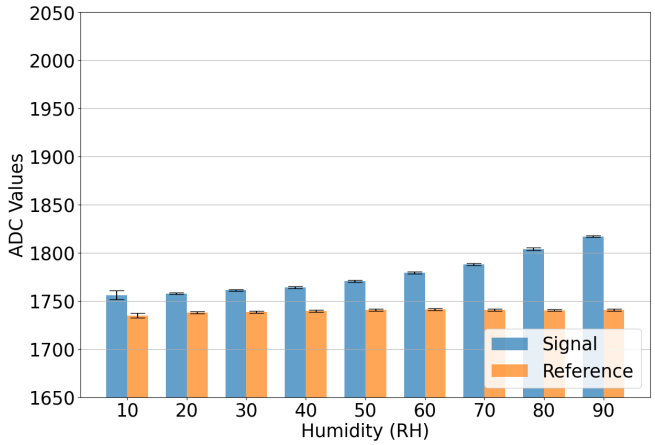

(a) Averages of signal and reference

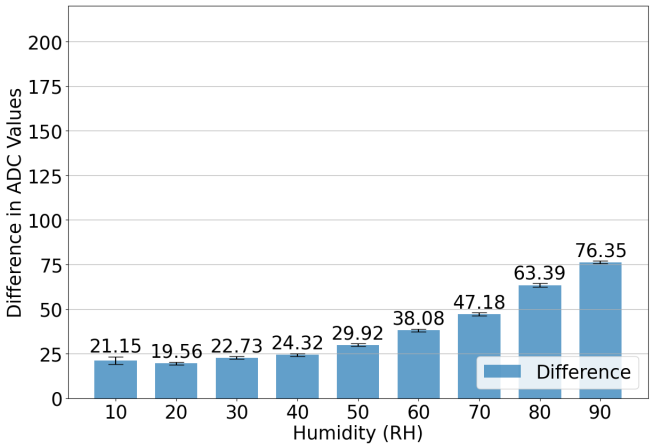

(b) Difference between signal and reference

Figure 5.12: Humidity measurements of a magenta inked chip.

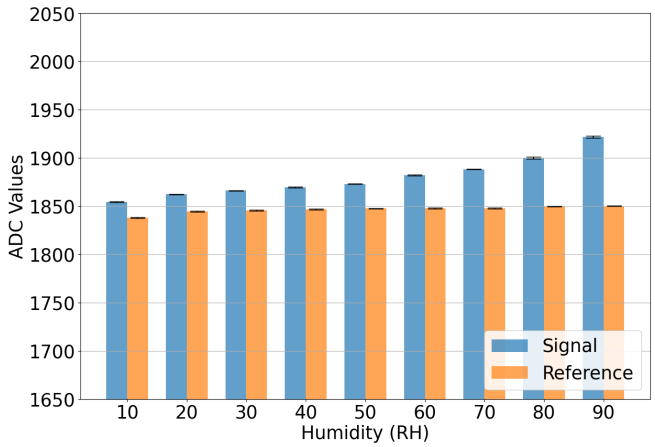

(a) Averages of signal and reference

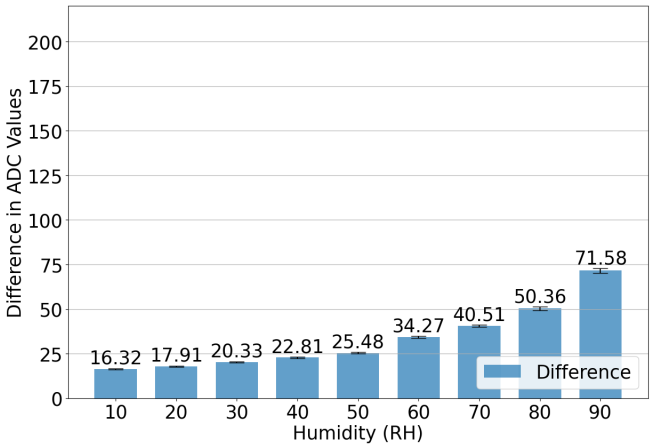

(b) Difference between signal and reference

Figure 5.13: Humidity measurements of a yellow inked chip.

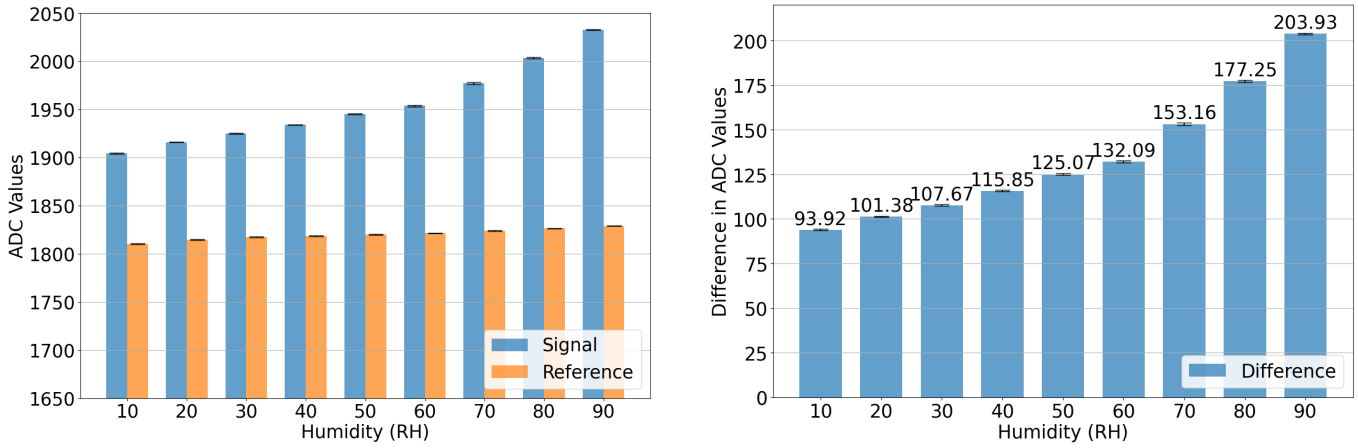

(a) Averages of signal and reference

(b) Difference between signal and reference

Figure 5.14: Humidity measurements of a grey inked chip.

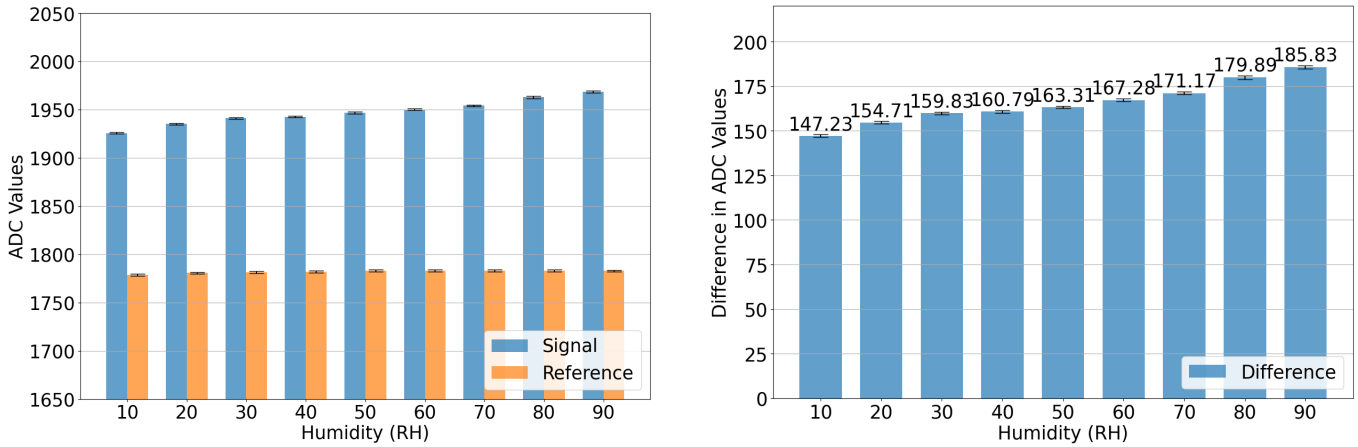

(a) Averages of signal and reference

(b) Difference between signal and reference

Figure 5.15: Humidity measurements of a black inked chip.

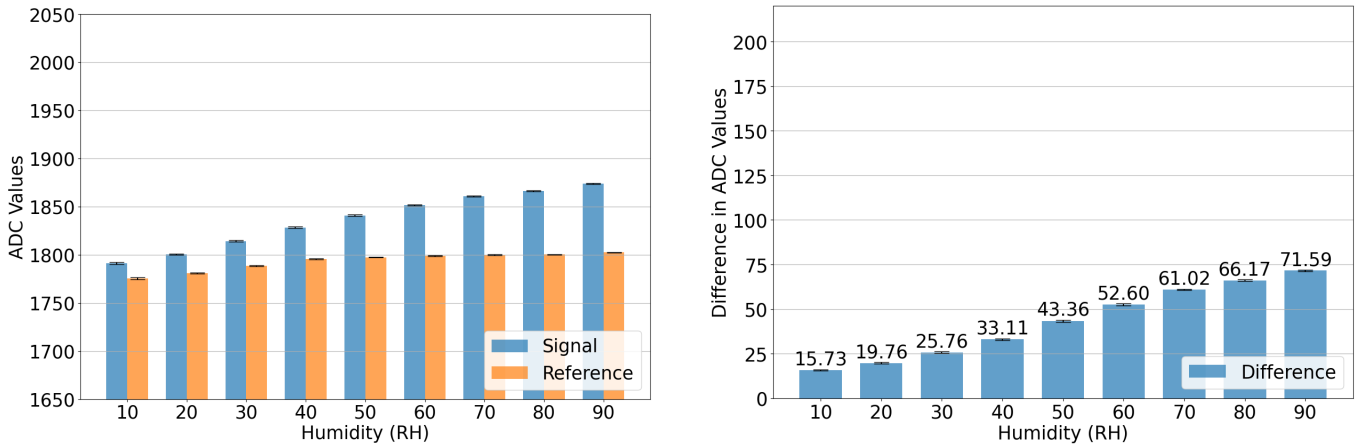

(a) Averages of signal and reference

(b) Difference between signal and reference

Figure 5.16: Humidity measurements of a photo-black inked chip.

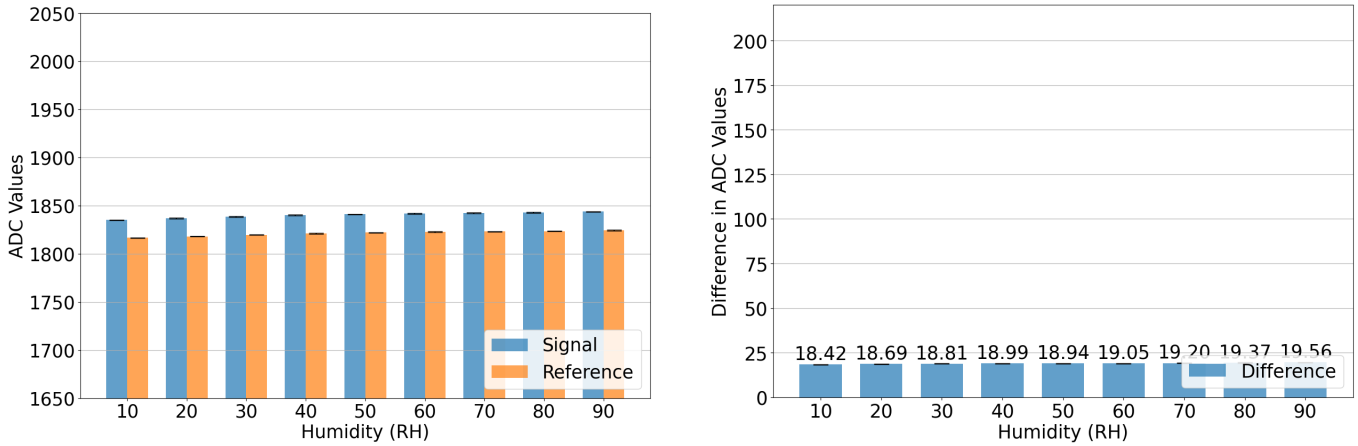

(a) Averages of signal and reference

(b) Difference between signal and reference

Figure 5.17: Humidity measurements of a white inked chip.

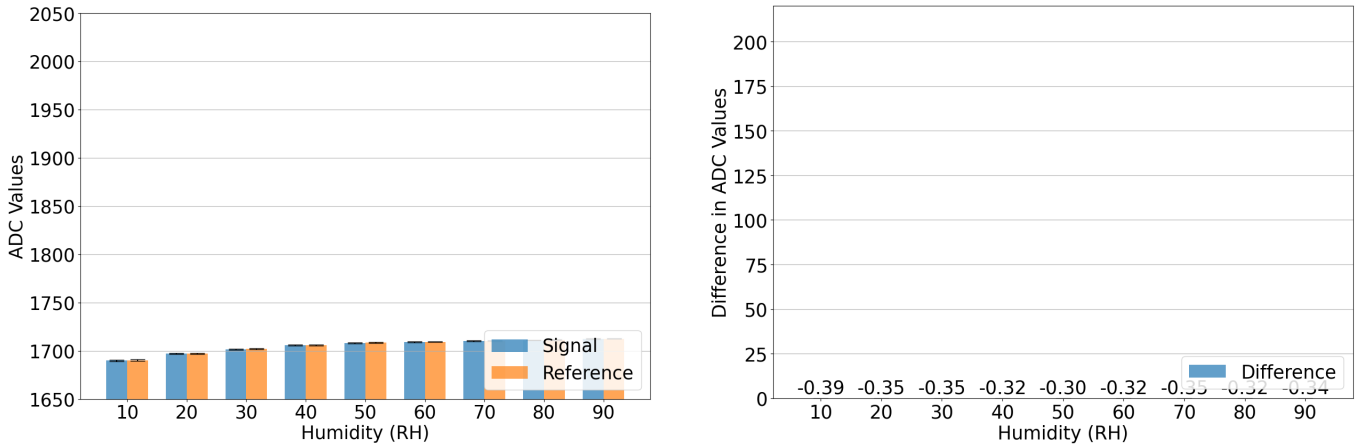

(a) Averages of signal and reference

(b) Difference between signal and reference

Figure 5.18: Humidity measurements of an empty chip.

5.2 Printed chips

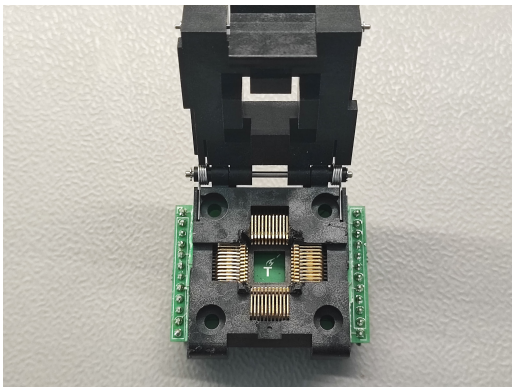

(a) PCB with clamshell socket

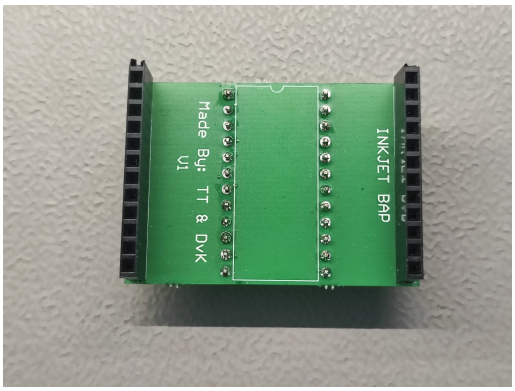

(b) Bottom PCB adapter

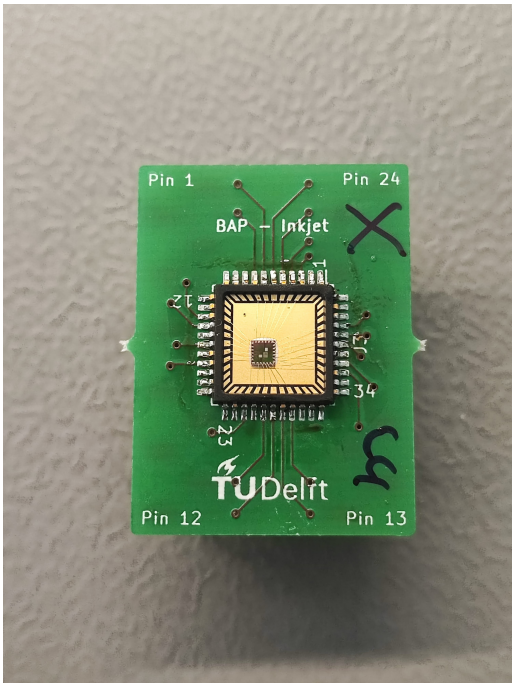

(c) Soldered chip on adapter

Figure 5.19: PCBs

The put together PCBs can be found in Figure 5.19. Both the soldered and the clamshell PCBs were succefully used to take measurements of the QFP44 packaged chips.

Grid with same sized dots

First, a grid with all the same sized dots was printed on the chip. Which was then soldered and measured. The results can be found in Figure 5.20. As can be seen the dots were successfully printed on the chip. Furthermore, the dots are reasonably distinguishable from the readout. The raster is not aimed and was printed over the entire chip.

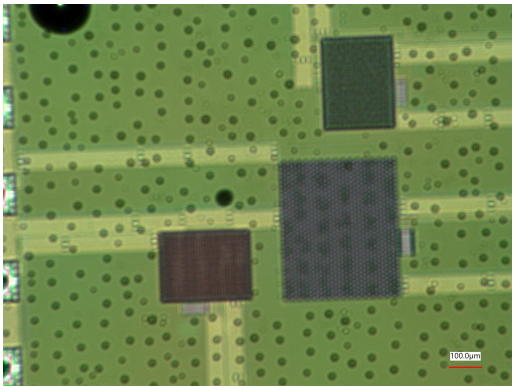

(a) Close-up of the printed chip, purposely unfocused to allow better observation of printed inks inside of the grid.

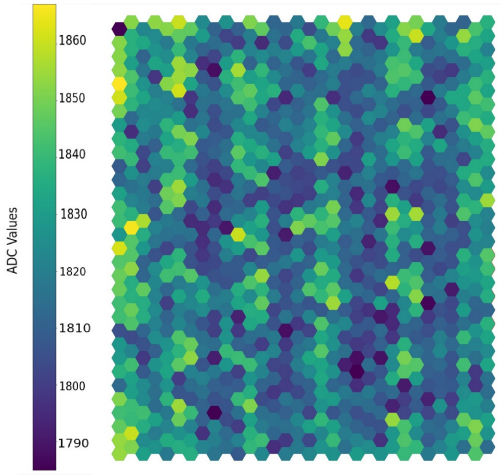

(b) Readout of the soldered chip

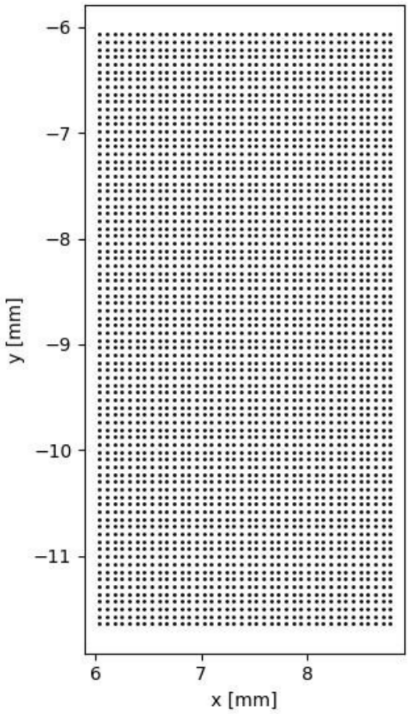

(c) Raster that was printed using the printer. Each dot has the same size

Figure 5.20: Printed chips

Grid with different sized dots.

A grid with variable dot thickness was printed on the chip. For this chip the printed raster was aimed only at the largest sensor grid. After printing, it was soldered on the PCB and read. A picture of the input raster, close-up of the chip and a readout can be found in Figure 5.21. Each dot has a different size, this was achieved by printing dots over each other, with the first dot being printed once in the smallest dot size, and the last dot being printed 16 times on the same spot. As can be seen, the measurements using the adapter were successful.

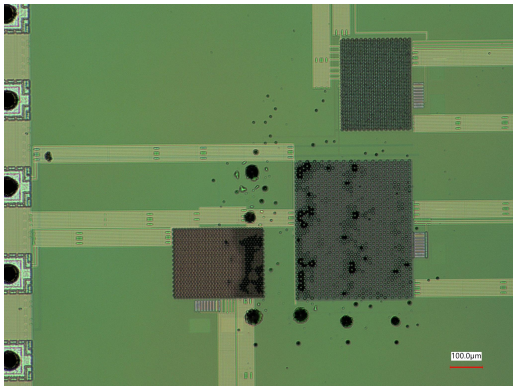

(a) Close-up of the printed chip

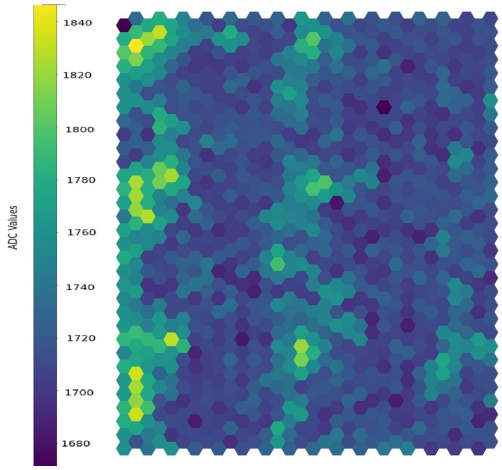

(b) Readout of the soldered chip

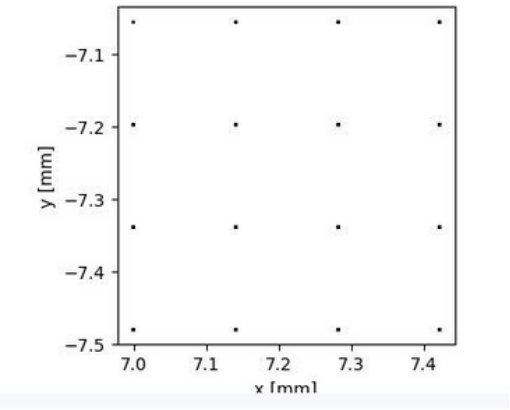

(c) Raster that was printed using the printer. Each dot has a different size

Figure 5.21: Printed chips

Multicoloured chip

In Figure 5.22 the results of the different coloured ink print is seen. Here the coloured raster was aimed to be over the largest grids. In the close-up it can be seen that different inks have been printed in on the chips, although it proved difficult to picture all colours. In the readout it is also difficult to visually distinguish as some inks increase the dielectric constant more than others. Therefore, these dots stand out.

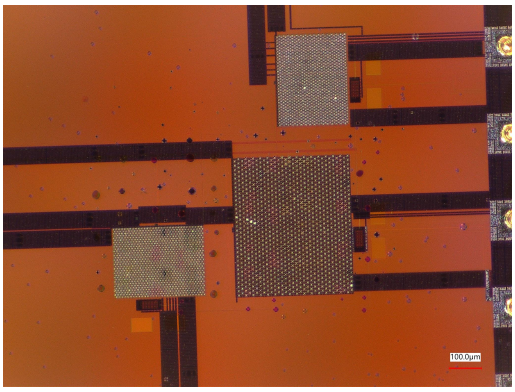

(a) Close-up of the printed chip

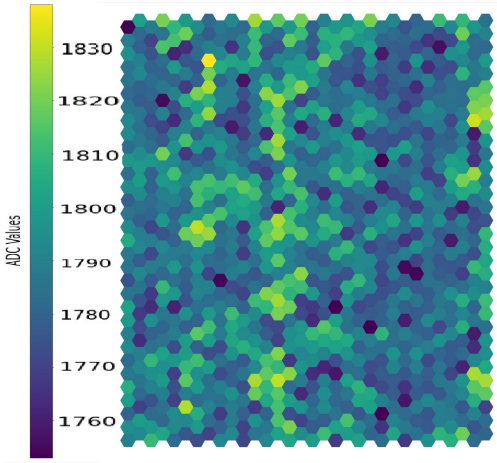

(b) Readout of the soldered chip

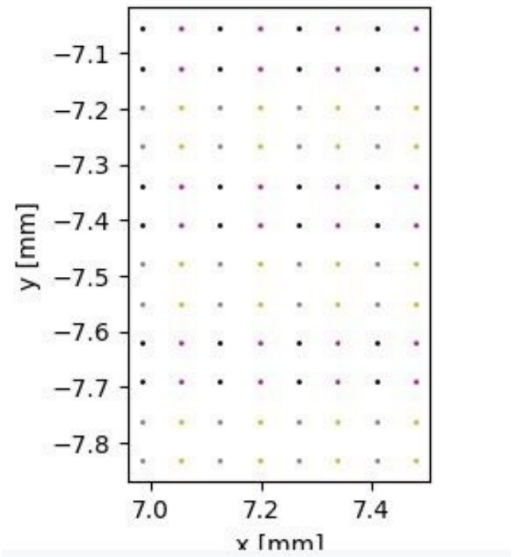

(c) Raster that was printed using the printer. Repeating pattern with different dot colours.

Figure 5.22: Multicoloured printed chip

Various Thickness

A chip with various thicknesses was printed the results can be found in Figure 5.23 Where thicker chips have a higher readout and are more sensitive to humidity changes.

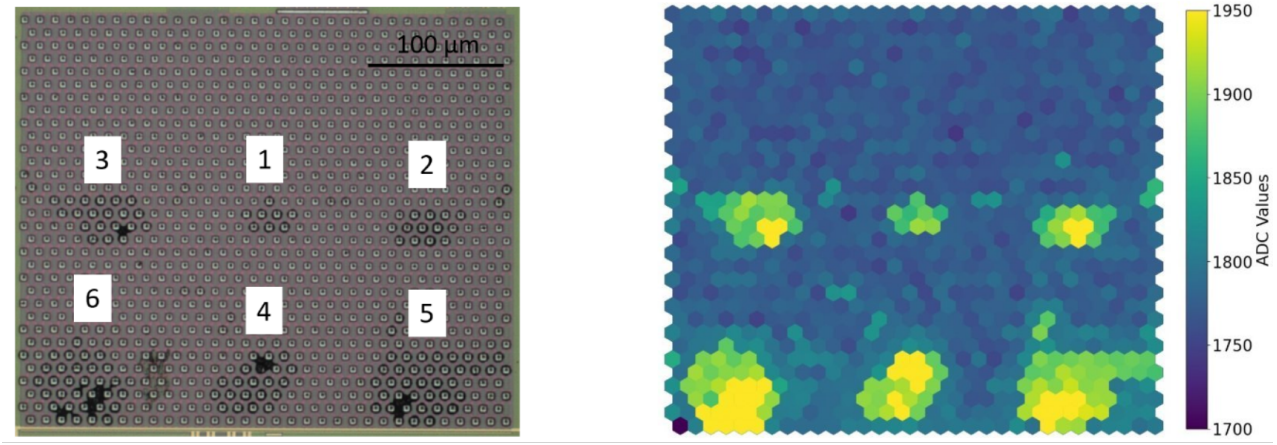

(a) Left, chip with various droplet sizes. The number indicating how many drops were dropped on the spot. Right showing the readout showing higher values for thicker inked spots.

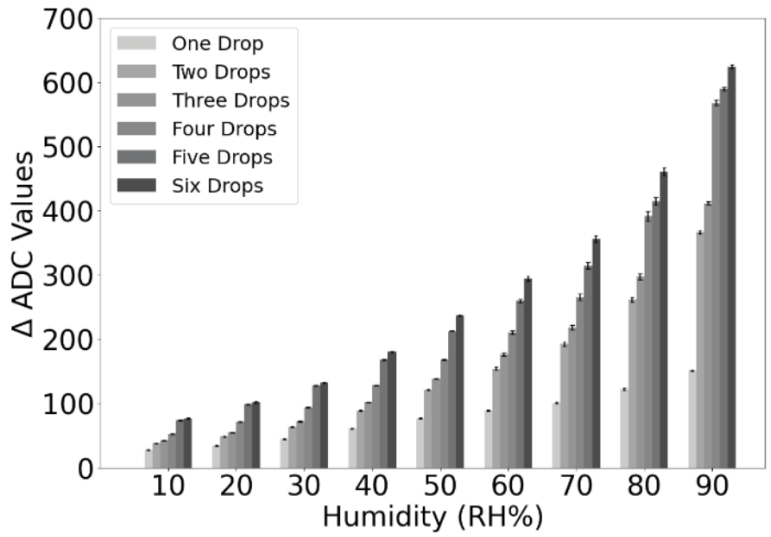

(b) Graph showing values of different thicknesses through relative humidity

Figure 5.23: Multi thickness chip

Various Colours

A chip was printed with various colours the results can be seen in Figure 5.24 here it can be seen that various inks have different responses on the same chip. Demonstrating the possibility of various sensing materials on one chip.

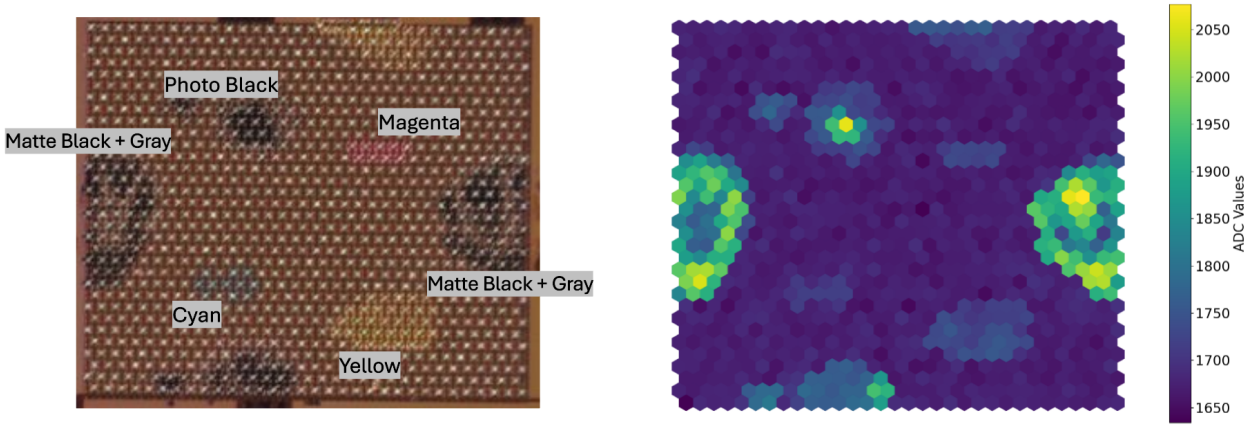

(a) Left, chip with various droplet colours. Right showing the readout.

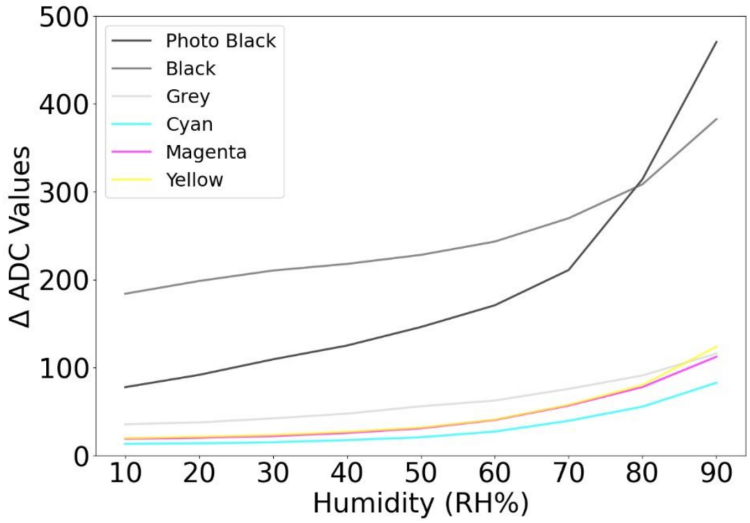

(b) Graph showing values of different colours through relative humidity

Figure 5.24: Multicoloured chip

6

Machine Learning

6.1 Introduction

As previously mentioned, a high-resolution microscope is used to identify which electrode is inked and which isn't. However, this method can be impractical in some cases to identify which electrode is inked and which isn't. Not all users have access to such an expensive device, and sometimes the chip cannot be placed under a microscope. Therefore, it would be useful to have a model that can accurately predict which electrodes are painted with which color using the capacitive data. If each ink exhibits a unique enough behaviour, a machine learning model could be trained to accurately predict the status of the electrodes.

6.2 Model Design

The machine learning model should output the ink type of the electrode, which can be considered as multiple mutually exclusive classes. Thus, a multiclass classification model is required. Therefore, a neural network model, used as a multiclass classification model, was explored. For the loss function, cross-entropy loss was used. Cross-entropy loss is suitable for training classification models because it measures the difference between two distributions: the actual probability of class Y given data X, and the probability of Y given X as predicted by the current model. A lower loss indicates that the distributions are closer to each other, and therefore, we aim to minimise this loss.

6.3 Data Acquisition and Feature Extraction

Data is essential for training the neural network. This data is acquired by collecting measurements from inked electrodes, with each inked electrode generating a data point. As previously explained in the result chapter, the difference between the signal and reference is the most reliable parameter to showcase the characteristic behaviour of the ink in different environments. Therefore, the features are based only on the difference between the reference and the signal electrodes.

The features consist of the mean and standard deviation of the difference in each humidity and light measurements for each inked electrode. Temperature measurements were excluded because the data was unreliable. A light or humidity measurement consist of eight and nine

individual measurements, respectively. Each measurement produces two features, resulting in a total of 34 features per data point.

Each inked electrode creates a data point. Whether an electrode is inked or not is determined using a high-resolution microscope. An image produced by the microscope and a corresponding readout can be seen in Figure 4.1. The data is divided into three equal parts: training, validation, and testing. The training and validation datasets are used to develop the neural network, while the testing dataset serves as an independent dataset to evaluate the neural network's performance and prevent overfitting.

6.4 Results

The model, based on a neural network, achieved an accuracy of 99.12% on the test dataset. It is important to note that all uninked electrodes on the chips were used as reference. Only electrodes on the empty chip were included in the dataset to ensure the classification of empty electrodes.

The neural network is reapplied to all chips. These results are displayed in Appendix D to give an indication of its working. These images cannot be considered to be real results, because in these images, the neural network is applied on data that it was trained on.

A model was also tested on a printed multicoloured chip the result of this can be seen in Figure 6.1 where the edge colour of the electrode represents the predicted colour. It has difficulty distinguishing yellow and magenta because of their similar response to stimuli. Besides this unfortunately the matte black and gray merged yet the model was still able to predict that these inks are the ones present here. Its confusion matrix can be found in Figure 6.2.

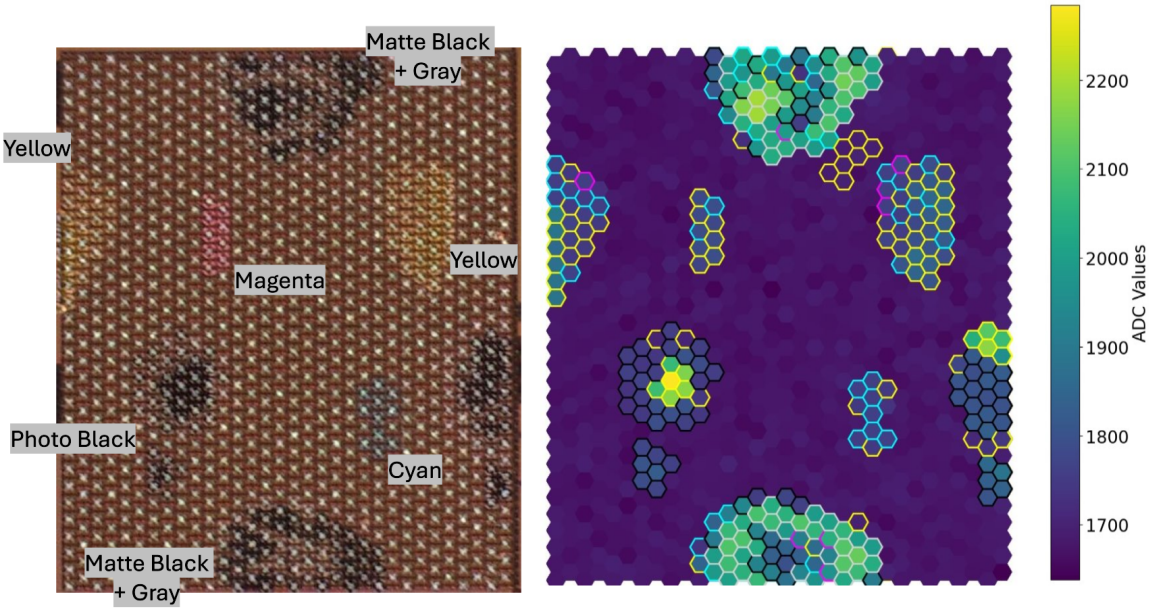

Figure 6.1: Multicoloured chip prediction

True

Predicted \ True	Cyan	Magenta	Yellow	P. Black	Uninked	Total
Cyan	7	2	15	0	0	24
Magenta	0	0	4	0	0	4
Yellow	3	7	37	15	8	70
P. Black	0	0	0	52	0	52
Uninked	1	0	1	0	750	752
Black	0	0	0	0	0	0
Gray	0	0	0	0	0	0
Total	11	9	57	67	758	902

Predicted

Figure 6.2: Confusion matrix the merged drops are left out.

7 Discussion

In the analysis of the relationship between humidity and capacitance for various inks, distinct patterns emerge. All water-based inks, except for black and photo black inks, exhibit an exponential relationship between humidity and capacitance. In contrast, the capacitance of white ink remains constant despite changes in humidity. This disparity highlights that the composition of water-based inks inherently fosters an exponential relationship with humidity.

The photo black ink displays a clear S-curve in response to humidity in Figure 5.16b. This is likely due to a dominant presence of carbon black in photo black ink, explained in Section 3.4.1. On the other hand, black ink shows a fluctuating linear relationship between humidity and capacitance in Figure 5.15b. This deviation from the expected exponential relationship could be attributed to a lower glycerol content, which can be seen in Table 3.1. Glycerol is known to induce exponential behaviour, as explained in Section 3.4.1. The observed linear relationship might result from a combination of a weaker exponential effect and an S-curve effect, ending at the lower percentages, caused by the carbon black present.

Our initial hypothesis was that light exposure would lead to an increase in the capacitance of the inks. Contrary to this expectation, the results indicate that light exposure generally causes a slight decrease in the capacitance of most inks, with the notable exceptions of white ink and black ink under ultraviolet light. The underlying mechanism for these decreases remains unclear. However, the unique behaviour of the white ink under light exposure might be attributed to its non-water solvent-based composition.

Furthermore, the grey and black chips exhibit a much higher response to both humidity and light measurements, indicating a high sensitivity.

7.1 Discussion of the Machine Learning Model

The machine learning model, based on a neural network using a cross-entropy loss function, is able to accurately identify most inked electrodes with the provided data. However, the neural network struggles to differentiate between empty electrodes and those with white ink. Notably, the neural network demonstrates an ability to identify inks that are difficult to discern even with a high-resolution microscope, as evidenced by the chip with yellow ink in Figure D.3.

Nevertheless, the dataset lacks sufficient variety in data sources. The neural network was trained, validated, and tested on inked electrodes from the same single chip, and there is no

evidence to suggest that the neural network would accurately identify inks on chips other than the eight used in this study. Therefore, it is recommended to significantly expand the dataset. However, mass production of data is not feasible with the drop-casting method. An inkjet printer is required for this purpose, highlighting the importance of having an inkjet printer.

In its current state, the machine learning model cannot reliably identify ink types or replace the microscope.

7.2 Future Recommendations

In the future, more tests should be done with different ink types. During this project the only ink that was not a standard Epson ink was the white ink. This ink proved difficult to work with as it was 1-ethoxy-2-(2-methoxyethoxy)ethane based and dissolved certain parts of the plastic of the housing of the printer. Besides that it also significantly degraded the tubes used for the inks. At the end of the project, two other inks were obtained. Both water based, one was a mixture of zinc oxide, blue ink and water and the other was a mixture of tin oxide, blue ink and water. Some rudimentary 365nm Uv measurements were done. These measurements can be found in Figure 7.1 & Figure 7.2. These are promising measurements as there are significant increases when the torch is turned on.

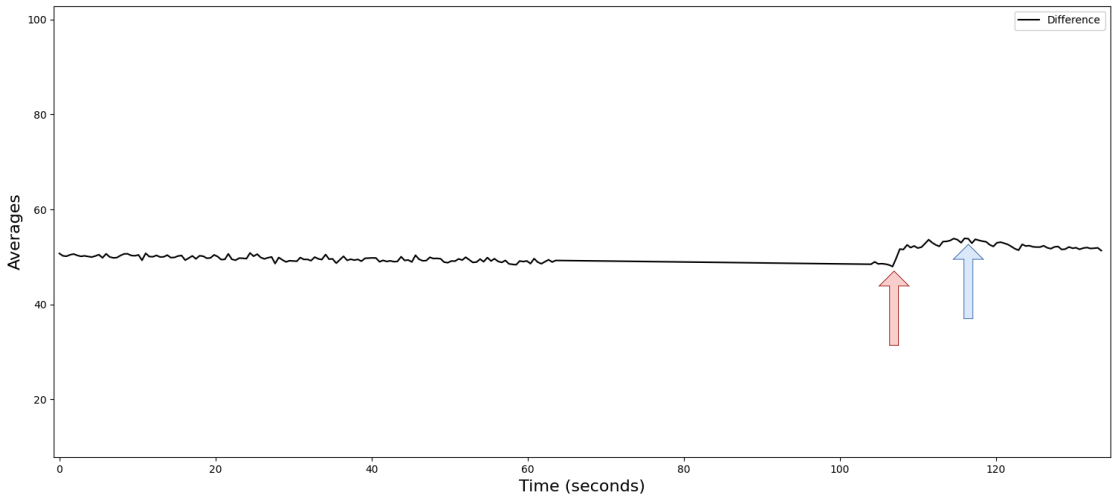

Figure 7.1: Mixture of Zinc Oxide, Cyan ink and water. Under 365nm torch, red arrows represent light on, blue represent light off. The straight line between 60 seconds and 105 seconds is where we paused the measurements and is not relevant for the phenomena.

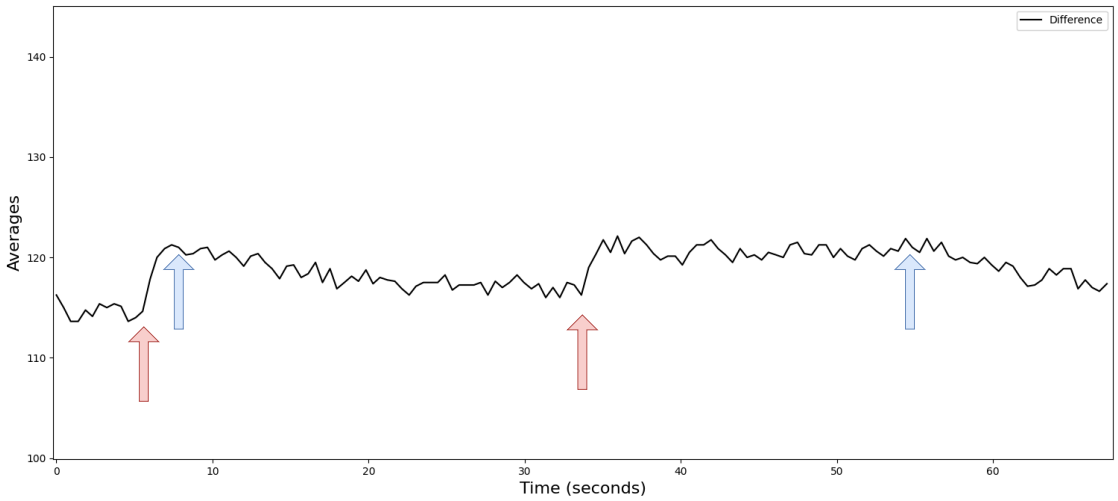

Figure 7.2: Mixture of Tin Oxide, Cyan ink and water. Under 365nm torch, red arrows represent light on, blue represent light off.

Besides this, for the temperature measurements an improved heating setup should be designed that is able to heat the chip while on the measurements board, this way the resulting data will be usable.

Finally, to increase the accuracy of the measurements of the light types, a light intensity detector should be used to ensure equal intensity across different light types.

8

Conclusions, recommendation and future work

Three measurement setups were developed to detect capacitance changes under varying conditions of humidity, light, and temperature. The setups dedicated to light and humidity measurements successfully generated usable data. However, the temperature setup requires redesigning to enable consistent chip temperature measurements. Furthermore, enhancing the light measurement setup with an intensity meter would standardize light intensity levels, thereby improving the reliability of the data.

In examining the relationship between humidity, light exposure, and capacitance across various ink formulations, several key insights have emerged. Water-based inks, excluding black and photo black variants, consistently exhibit an exponential relationship with humidity, while white ink demonstrates a stable capacitance profile regardless of humidity changes. This distinction underscores the inherent influence of ink composition on capacitance dynamics under varying environmental conditions. The presence of carbon black notably induces a S-curve response in photo black ink to humidity variations.

Contrary to our initial hypothesis, light exposure generally leads to a slight decrease in capacitance for most inks, except for white ink and black ink under ultraviolet light. The mechanism behind these trends remains unclear but could be linked to the solvent-based nature of white ink, influencing its response to light exposure.

The machine learning model, based on a neural network using a cross-entropy loss function, demonstrates effective identification of inked electrodes, although it struggles with distinguishing between empty electrodes and those with white ink. Notably, the neural network showcases proficiency in identifying subtle ink variations that are challenging to discern even with high-resolution microscopy. However, the model's training and validation were restricted to data sourced exclusively from a single chip, limiting its generalizability to other chips. To enhance robustness, future efforts should focus on expanding the dataset to encompass diverse ink types and chip sources. Notably, the integration of an inkjet printer would facilitate the acquisition of a broader dataset, crucial for refining the model's accuracy and applicability.

This means that Requirement [1.1] is fulfilled for humidity, could be improved for Light and has to be redesigned for Temperature. Requirements [1.2] & [1.3] have been fulfilled as we were able to read data from the adapter which we were then able to interpret using a python program. [2.1] has been completed, although an intensity detector should be added for added accuracy, [2.2] has been successfully completed, [2.3] has been partially completed as the main influence of temperature has been found the measurement setup produces inaccurate data as we did not preserve the chip's heat. [2.4] has not been succesfully completed. A machine learning classification model has been made, but due to a lack of diversity in data, the model is inadequate.

References

[1] Muhammad Ali Shah et al. "Classifications and Applications of Inkjet Printing Technology: A Review". In: *IEEE Access* 9 (2021), pp. 140079–140102. DOI: 10.1109/ACCESS.2021.3119219. URL: http://dx.doi.org/10.1109/ACCESS.2021.3119219 (visited on 04/23/2024).

[2] Rick Waasdorp et al. "Accessing individual 75-micron diameter nozzles of a desktop inkjet printer to dispense picoliter droplets on demand". In: *RSC Adv.* 8 (27 2018), pp. 14765–14774. DOI: 10.1039/C8RA00756J. URL: http://dx.doi.org/10.1039/C8RA00756J (visited on 04/23/2024).

[3] Daniel J. Cohen, Roberto C. Morfino, and Michel M. Maharbiz. "A Modified Consumer Inkjet for Spatiotemporal Control of Gene Expression". In: *PLOS ONE* 4.9 (Sept. 2009), pp. 1–8. DOI: 10.1371/journal.pone.0007086. URL: https://doi.org/10.1371/journal.pone.0007086 (visited on 04/24/2024).

[4] Nikolaj Kofoed Mandsberg et al. "Consumer-Grade Inkjet Printer for Versatile and Precise Chemical Deposition". In: *ACS Omega* 6.11 (2021). PMID: 33778290, pp. 7786–7794. DOI: 10.1021/acsomega.1c00282. eprint: https://doi.org/10.1021/acsomega.1c00282. URL: https://doi.org/10.1021/acsomega.1c00282 (visited on 04/24/2024).

[5] Hanjin Cho, M. (Ash) Parameswaran, and Hua-Zhong Yu. "Fabrication of microsensors using unmodified office inkjet printers". In: *Sensors and Actuators B: Chemical* 123.2 (2007), pp. 749–756. ISSN: 0925-4005. DOI: https://doi.org/10.1016/j.snb.2006.10.022. URL: https://www.sciencedirect.com/science/article/pii/S0925400506006952.

[6] Frans Widdershoven et al. "A CMOS Pixelated Nanocapacitor Biosensor Platform for High-Frequency Impedance Spectroscopy and Imaging". In: *IEEE Transactions on Biomedical Circuits and Systems* 12.6 (2018), pp. 1369–1382. DOI: 10.1109/TBCAS.2018.2861558.

[7] S. G. Lemay et al. "High-frequency nanocapacitor arrays: concept, recent developments, and outlook". In: *Accounts of Chemical Research* 49 (10 2016), pp. 2355–2362. DOI: 10.1021/acs.accounts.6b00349.

[8] C. Laborde et al. "Real-time imaging of microparticles and living cells with cmos nanocapacitor arrays". In: *Nature Nanotechnology* 10 (9 2015), pp. 791–795. DOI: 10.1038/nnano.2015.163.

[9] A. Moya et al. "Inkjet-printed electrochemical sensors". In: *Current Opinion in Electrochemistry* 3 (1 2017), pp. 29–39. DOI: 10.1016/j.coelec.2017.05.003.

[10] N. Lazarus et al. "Cmos-mems capacitive humidity sensor". In: *Journal of Microelectromechanical Systems* 19 (1 2010), pp. 183–191. DOI: 10.1109/jmems.2009.2036584.

[11] Stephen Brunauer et al. "On a theory of the van der Waals adsorption of gases". In: *Journal of the American Chemical society* 62.7 (1940), pp. 1723–1732.

[12] M. Mathlouthi and B. Rogé. "Water vapour sorption isotherms and the caking of food powders". In: *Food Chemistry* 82 (1 2003), pp. 61–71. DOI: 10.1016/s0308-8146(02)00534-4.

[13] B. Saberi et al. “Water sorption isotherm of pea starch edible films and prediction models”. In: *Foods* 5 (1 2015), p. 1. DOI: 10.3390/foods5010001.

[14] Kazuhiko et. al. Kitamure and Seiko Epson Corp. *US7416592B2 - Magenta ink composition, ink set, ink cartridge, inkjet recording method and recorded product*. en. Aug. 2008. URL: https://patents.google.com/patent/US7416592B2/en.

[15] J. Raymond et. al. Adamic and Hewlett Packard Development Co LP. *US6607589B2 - Cyan ink formulation*. en. July 2003. URL: https://patents.google.com/patent/US6607589B2/en.

[16] Kazuhiko Kitamura, Akihito Sao, and Seiko Epson Corp. *EP2048204B1 - Yellow ink composition, ink set, ink cartridge, inkjet recording method and recorded matter - Google Patents*. en. Apr. 2012. URL: https://patents.google.com/patent/EP2048204B1/en.

A

Tables

A.1 Light Measurements

Cyan

Table A.1: The mean and standard deviation of the signal, reference and difference of the light measurements of the cyan chip.

File Name	Signal	SD	Reference	SD	Difference	SD
Dark	1861.56	0.62	1791.29	0.65	70.28	0.30
White	1860.31	0.60	1791.99	0.58	68.32	0.37
Blue	1860.56	0.62	1792.94	0.71	67.62	0.34
Green	1859.37	0.72	1792.28	0.70	67.08	0.33
Red	1859.71	0.60	1792.95	0.62	66.76	0.31
UV 255	1859.34	0.70	1792.63	0.55	66.71	0.48
UV 310	1857.12	0.74	1793.22	0.58	63.90	0.47
UV 365	1863.49	0.62	1809.36	0.93	54.13	0.48

Magenta

Table A.2: The mean and standard deviation of the signal, reference and difference of the light measurements of the magenta chip.

File Name	Signal	SD	Reference	SD	Difference	SD
Dark	1817.82	0.99	1740.41	0.97	77.41	0.73
White	1816.09	1.07	1740.11	1.03	75.98	0.66
Blue	1815.55	1.04	1741.46	1.08	74.08	0.75
Green	1814.94	1.00	1741.37	1.01	73.58	0.70
Red	1814.48	0.90	1741.22	0.95	73.26	0.77
UV 255	1812.60	1.08	1740.70	1.03	71.89	0.82
UV 310	1810.05	0.94	1740.44	1.00	69.61	0.76
UV 365	1815.92	0.93	1756.39	1.36	59.53	0.88

Yellow

Table A.3: The mean and standard deviation of the signal, reference and difference of the light measurements of the yellow chip.

File Name	Signal	SD	Reference	SD	Difference	SD
Dark	1873.65	0.37	1844.71	0.78	28.94	0.67
White	1872.44	0.44	1846.04	0.51	26.40	0.48
Blue	1871.64	0.46	1846.39	0.45	25.24	0.39
Green	1871.77	0.50	1846.71	0.48	25.06	0.32
Red	1870.84	0.50	1845.65	0.51	25.19	0.30
UV 255	1869.95	0.49	1844.32	0.48	25.63	0.32
UV 310	1869.92	0.58	1844.77	0.52	25.15	0.34
UV 365	1872.35	0.93	1851.26	1.38	21.09	0.55

Grey

Table A.4: The mean and standard deviation of the signal, reference and difference of the light measurements of the grey chip.

File Name	Signal	SD	Reference	SD	Difference	SD
Dark	1973.91	0.48	1821.71	0.40	152.20	0.45
White	1970.95	0.59	1822.07	0.52	148.88	0.60
Blue	1969.70	0.49	1822.77	0.40	146.93	0.49
Green	1969.22	0.50	1823.02	0.55	146.21	0.35
Red	1969.18	0.49	1823.17	0.41	146.01	0.39
UV 255	1969.91	0.41	1822.81	0.44	147.09	0.36
UV 310	1969.17	1.52	1822.50	1.17	146.66	0.60
UV 365	1962.12	0.76	1823.87	2.19	138.25	1.70

Black

Table A.5: The mean and standard deviation of the signal, reference and difference of the light measurements of the black chip.

File Name	Signal	SD	Reference	SD	Difference	SD
Dark	1944.81	0.88	1782.23	1.00	162.59	0.80
White	1945.66	1.01	1783.88	1.20	161.78	0.77
Blue	1945.93	0.98	1784.57	1.07	161.35	0.68
Green	1946.04	1.05	1784.61	1.17	161.43	0.73
Red	1946.39	0.80	1784.96	0.85	161.43	0.65
UV 255	1946.74	0.94	1784.76	1.01	161.98	0.81
UV 310	1947.95	1.05	1785.21	1.22	162.74	0.75
UV 365	1958.75	1.44	1795.00	1.19	163.75	0.79

Photo Black

Table A.6: The mean and standard deviation of the signal, reference and difference of the light measurements of the photo black chip.

File Name	Signal	SD	Reference	SD	Difference	SD
Dark	1835.74	0.57	1794.17	0.53	41.57	0.30
White	1837.27	0.48	1797.19	0.69	40.08	0.41
Blue	1838.42	0.40	1800.00	0.44	38.42	0.37
Green	1838.79	0.39	1799.94	0.41	38.85	0.34
Red	1839.00	0.60	1800.26	0.59	38.75	0.31
UV 255	1838.99	0.39	1800.18	0.39	38.82	0.31
UV 310	1840.00	0.53	1802.29	0.69	37.72	0.38
UV 365	1848.72	2.63	1819.02	3.73	29.69	1.16

White Ink

Table A.7: The mean and standard deviation of the signal, reference and difference of the light measurements of the white chip.

File Name	Signal	SD	Reference	SD	Difference	SD
Dark	1843.62	0.58	1824.75	0.58	18.87	0.15
White	1843.61	0.34	1824.75	0.33	18.87	0.15
Blue	1843.58	0.34	1824.72	0.35	18.86	0.16
Green	1842.83	0.45	1824.05	0.46	18.77	0.15
Red	1842.48	0.35	1823.77	0.39	18.71	0.17
UV 255	1844.28	0.37	1823.78	0.37	20.50	0.16
UV 310	1844.36	0.38	1823.92	0.40	20.44	0.16
UV 365	1858.65	0.85	1838.19	0.86	20.46	0.16

Empty

Table A.8: The mean and standard deviation of the signal, reference and difference of the light measurements of the empty chip.

File Name	Signal	SD	Reference	SD	Difference	SD
Dark	1719.47	0.41	1719.78	0.49	-0.31	0.39
White	1720.93	0.50	1721.25	0.52	-0.32	0.38
Blue	1721.96	0.52	1722.27	0.51	-0.31	0.43
Green	1721.46	0.43	1721.87	0.47	-0.41	0.40
Red	1720.81	0.43	1721.15	0.44	-0.34	0.40
UV 255	1720.53	0.42	1720.79	0.47	-0.26	0.37
UV 310	1721.52	0.42	1721.84	0.48	-0.32	0.39
UV 365	1740.79	1.33	1741.03	1.35	-0.25	0.32

A.2 Moisture Measurements

Cyan

Table A.9: The mean and standard deviation of the signal, reference and difference of the moisture measurements of the cyan chip.

File Name	Signal	SD	Reference	SD	Difference	SD
10	1807.98	0.71	1782.02	0.66	25.96	0.39
20	1815.95	0.79	1786.76	0.82	29.19	0.31
30	1821.49	0.62	1788.83	0.62	32.66	0.34
40	1812.97	0.70	1786.24	0.69	26.73	0.27
50	1835.12	0.82	1791.53	0.68	43.60	0.44
60	1843.63	0.99	1792.24	0.58	51.39	0.85
70	1854.67	0.82	1792.02	0.63	62.65	0.81
80	1859.87	1.01	1790.95	0.60	68.92	0.87
90	1872.31	0.69	1792.79	0.63	79.53	0.44

Magenta

Table A.10: The mean and standard deviation of the signal, reference and difference of the moisture measurements of the magenta chip.

File Name	Signal	SD	Reference	SD	Difference	SD
10	1756.10	4.48	1734.95	2.62	21.15	2.11
20	1757.70	0.88	1738.14	1.07	19.56	0.81
30	1761.15	0.96	1738.42	1.01	22.73	0.68
40	1764.04	0.93	1739.72	1.03	24.32	0.83
50	1770.58	1.00	1740.66	1.10	29.92	0.68
60	1779.34	1.24	1741.26	1.05	38.08	0.78
70	1787.96	1.14	1740.78	0.93	47.18	0.86
80	1803.79	1.36	1740.40	1.06	63.39	1.02
90	1817.07	0.99	1740.72	1.03	76.35	0.69

Yellow

Table A.11: The mean and standard deviation of the signal, reference and difference of the moisture measurements of the yellow chip.

File Name	Signal	SD	Reference	SD	Difference	SD
10	1854.44	0.52	1838.12	0.46	16.32	0.36
20	1862.36	0.38	1844.46	0.41	17.91	0.32
30	1866.10	0.47	1845.77	0.48	20.33	0.34
40	1869.64	0.37	1846.83	0.36	22.81	0.36
50	1873.12	0.37	1847.64	0.41	25.48	0.42
60	1882.02	0.53	1847.75	0.43	34.27	0.54
70	1888.32	0.43	1847.81	0.42	40.51	0.55
80	1900.13	0.97	1849.77	0.43	50.36	0.95
90	1921.80	1.26	1850.23	0.45	71.58	1.30

Grey

Table A.12: The mean and standard deviation of the signal, reference and difference of the moisture measurements of the grey chip.

File Name	Signal	SD	Reference	SD	Difference	SD
10	1904.22	0.61	1810.30	0.47	93.92	0.41
20	1916.03	0.44	1814.65	0.34	101.38	0.37
30	1924.92	0.57	1817.25	0.48	107.67	0.49
40	1934.24	0.34	1818.39	0.39	115.85	0.33
50	1945.35	0.44	1820.27	0.48	125.07	0.51
60	1953.66	0.81	1821.56	0.39	132.09	0.61
70	1977.34	1.06	1824.18	0.54	153.16	0.79
80	2003.62	0.64	1826.37	0.46	177.25	0.57
90	2032.96	0.60	1829.03	0.34	203.93	0.47

Black

Table A.13: The mean and standard deviation of the signal, reference and difference of the moisture measurements of the black chip.

File Name	Signal	SD	Reference	SD	Difference	SD
10	1925.84	0.99	1778.61	1.09	147.23	0.76
20	1935.38	0.81	1780.67	1.02	154.71	0.71
30	1941.15	0.95	1781.31	1.06	159.83	0.74
40	1942.64	0.93	1781.85	1.03	160.79	0.79
50	1946.60	1.09	1783.29	1.11	163.31	0.70
60	1950.25	0.91	1782.98	0.98	167.28	0.78
70	1954.30	0.89	1783.13	0.98	171.17	0.73
80	1962.90	1.19	1783.02	0.93	179.89	1.06
90	1968.80	1.04	1782.96	0.94	185.83	0.91

Photo Black

Table A.14: The mean and standard deviation of the signal, reference and difference of the moisture measurements of the photo black chip.

File Name	Signal	SD	Reference	SD	Difference	SD
10	1791.31	1.23	1775.59	1.13	15.73	0.36
20	1800.59	0.56	1780.82	0.61	19.76	0.36
30	1814.37	0.61	1788.61	0.59	25.76	0.37
40	1828.51	0.75	1795.40	0.55	33.11	0.44
50	1840.88	0.77	1797.51	0.50	43.36	0.59
60	1851.65	0.70	1799.05	0.45	52.60	0.54
70	1861.13	0.53	1800.11	0.46	61.02	0.34
80	1866.49	0.51	1800.32	0.48	66.17	0.43
90	1874.10	0.52	1802.51	0.46	71.59	0.33

White Ink

Table A.15: The mean and standard deviation of the signal, reference and difference of the moisture measurements of the white chip.

File Name	Signal	SD	Reference	SD	Difference	SD
10	1835.11	0.37	1816.69	0.40	18.42	0.15
20	1836.84	0.44	1818.16	0.45	18.69	0.15
30	1838.62	0.49	1819.81	0.49	18.81	0.14
40	1840.17	0.37	1821.18	0.37	18.99	0.14
50	1841.10	0.39	1822.16	0.37	18.94	0.16
60	1841.89	0.41	1822.84	0.41	19.05	0.15
70	1842.38	0.35	1823.18	0.38	19.20	0.16
80	1842.99	0.43	1823.61	0.43	19.37	0.16
90	1843.89	0.40	1824.33	0.41	19.56	0.13

Empty

Table A.16: The mean and standard deviation of the signal, reference and difference of the moisture measurements of the empty chip.

File Name	Signal	SD	Reference	SD	Difference	SD
10	1689.93	0.97	1690.32	0.96	-0.39	0.32
20	1697.02	0.49	1697.37	0.48	-0.35	0.38
30	1701.52	0.51	1701.87	0.58	-0.35	0.39
40	1705.82	0.49	1706.14	0.54	-0.32	0.37
50	1708.13	0.46	1708.43	0.49	-0.30	0.35
60	1709.09	0.46	1709.41	0.48	-0.32	0.38
70	1710.13	0.44	1710.48	0.46	-0.35	0.37
80	1710.97	0.35	1711.29	0.46	-0.32	0.34
90	1712.29	0.40	1712.63	0.43	-0.34	0.37

B

Temperature Measurements

Temperature
As the temperature increases, the molecules of the dielectric start to move vigorously. This means that it is harder for the molecules to polarize. And therefore the dielectric constant of the material drops.

B.1 Measurement Setup

A hot plate was used to increase the temperature of the chip surface. Chips were placed on the hot plate upside down for more direct heat transfer. A hot plate cannot cool the chip. So only measurements above room temperature were measured. The hot plate would be set to a temperature between 30 and 80 degrees Celsius. The chips were given 10 minutes to reach the desired temperature. Afterwards, they were removed from the plate and put in the measurement board and a measurement was taken. An illustration of the measurement setup can be seen in Figure B.1

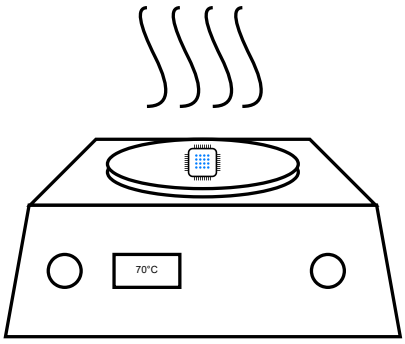

Figure B.1: An illustration of the temperature measurement setup.

B.2 Results

Table B.1: Measurements Yellow dots with Varying Temperatures

Temperature (C)	Signal	SD	Reference	SD	Difference	SD
30	1887.07	0.55	1845.12	0.44	41.95	0.65
40	1887.36	0.30	1851.48	0.45	35.88	0.36
50	1890.73	0.41	1857.11	0.43	33.61	0.33
60	1895.14	0.44	1862.58	0.48	32.56	0.25
70	1898.73	0.46	1867.40	0.50	31.33	0.25
80	1906.83	0.73	1876.23	0.78	30.60	0.15

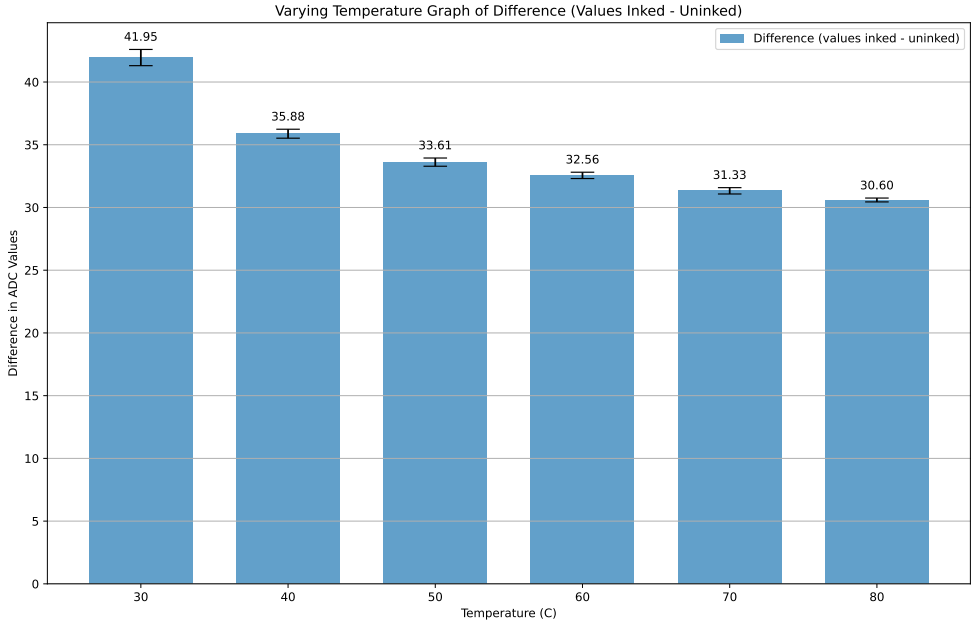

Figure B.2: Difference Graph Yellow Dots (B4)

Table B.2: Measurements Photo Black Dots with Varying Temperatures

Temperature (C)	Signal	SD	Reference	SD	Difference	SD
30	1840.08	1.49	1812.63	0.49	27.44	1.53
40	1848.99	0.37	1827.96	0.31	21.03	0.23
50	1861.06	0.43	1842.04	0.45	19.02	0.26
60	1871.08	0.52	1853.58	0.63	17.51	0.24
70	1879.25	0.74	1862.42	0.73	16.83	0.17
80	1900.28	0.90	1883.69	0.89	16.59	0.15

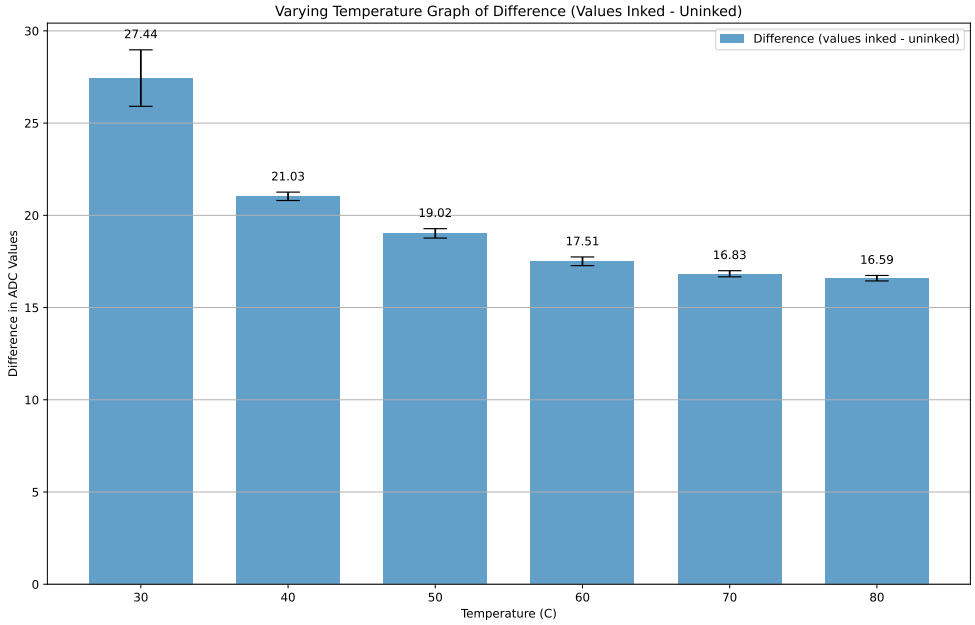

Figure B.3: Difference Graph Photo Black Dots (B6)

The ADC values from both the inked signal spots and the reference spots are increasing with the temperature. But the inked electrodes rise slower than the uninked electrodes, therefore the difference between their values gets gradually lower. The difference can also be seen in Figure B.2

B.3 Problem with the measurements setup

After heating the chips and placing them in the unheated measurements board, the temperature would rapidly drop. This would cause the measurements to be unreliable as any delay in inserting the chips would drastically alter the read-out values. Ideally, we would need to heat the chip when already in the socket and measure the temperature using a probe.

However, a trend of decreasing difference with higher temperature could be noted. Nonetheless, it not possible to draw conclusions as the measurement technique and therefore the data was flawed.

C

Derivations & compositions

C.1 Switched Capacitor

$$C = \frac{Q}{V} \tag{C.1}$$

Where

- C is the capacitance (F),
- Q is charge (C),
- V is voltage (V),

and

$$I = \frac{Q}{s} \tag{C.2}$$

- I is Current (A),
- Q is charge (C),
- s is seconds (s),

Every cycle a charge goes into the electrode which can be calculated as

$$q_{in} = CV_{dd}$$

and every cycle a charge leaves the electrode which can be calculated as

$$q_{out} = CV_{out}$$

.

Therefore, the

$$\Delta q = C(V_{dd} - V_{out})$$

combining this with Equation C.1 results in

$$I = C(V_{dd} - V_{out})f$$

where

- f is the Frequency (Hz)

In our case V_{out} is ground therefore this equation reduces to

$$I = CV_{dd}f \tag{C.3}$$

C.2 Ink Composition

Magenta

A magenta ink composition used as a colorant, containing at least one type of compound represented by Formula (I) below and at least one type of compound represented by Formula (II) below:

Magenta ink Composition containing at least one type of compound represented by Figure C.1.a and one type of compound represented by Figure C.1.b.[14]

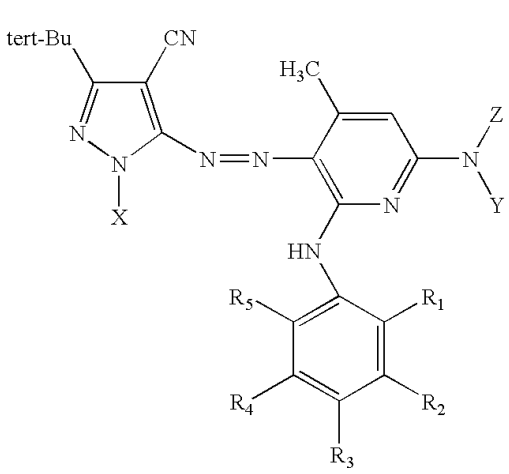

(a) "R1 to R5 represent a hydrogen atom, alkyl group, or a sulfo group or salt thereof; and independently R1 and R5 may be optionally substituted provided both are alkyl groups and the total number of carbon atoms constituting those alkyl groups is 3 or more"[14]

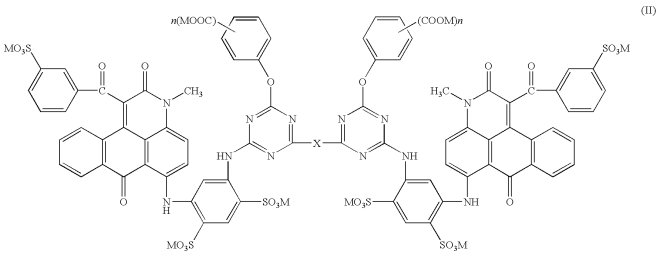

(b) "R1 to R10 represent a hydrogen atom, alkyl group, or a sulfo group or salt thereof; independently (R1 and R5) and (R6 and R10) may be optionally substituted provided both are alkyl groups and the total number of carbon atoms constituting those alkyl groups is 3 or more; and M represents a hydrogen atom or alkaline metal atom"[14]

Figure C.1: Compounds magenta inks

Cyan

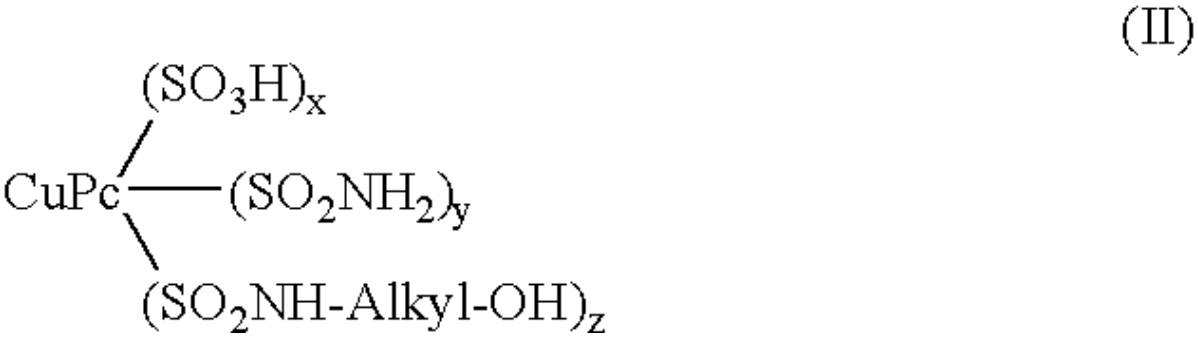

Figure C.2: Cyan Chemical Formula from patent, where X, Y, Z = 4 & CuPc is Copper Phtalocyanine[15]

Yellow

The yellow colourant contains at least one type of [C3] and one type of [C2][16]

[C3]

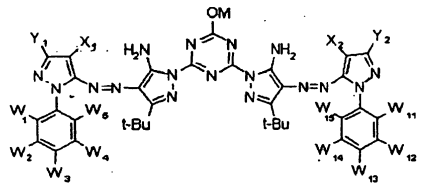

(I I I)

(a) "X1, X2, Y1, and Y2 are each a hydrogen atom or a cyano group, W1 to W5 and W11 to W15 are each a hydrogen atom or a carboxyl group or salt thereof, M is a metal atom, and t-Bu is a tertiary butyl group"[16]

[C2]

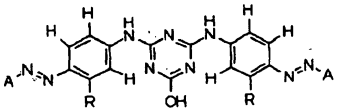

(I I)

(b) "R is a methoxy group or methyl group, and A is 1,5-disulfonaphtho-3-yl or 1,5,7. trisulfonaphtho-2-yl."[16]

Figure C.3: Compounds Yellow inks

D

Machine Learning Images

D.1 Images of Ink Predictions

The developed machine learning model was reapplied to the chips. The resulting predictions are displayed in Figures D.1 to D.8. In these figures, the predicted inks on the electrodes are shown alongside images obtained from a microscope. In the machine learning prediction images, each electrode is represented by a hexagon. The outline color of the hexagon indicates the color predicted by the model, while the absence of an outline indicates that the model predicted an empty electrode. The center color of each hexagon represents the ADC value of the chip measurement at 90% relative humidity, providing better visualization of the inked parts through contrast in the data.

It is important to note that these images cannot be considered as real results, as the model was reapplied to the same data it was trained on.

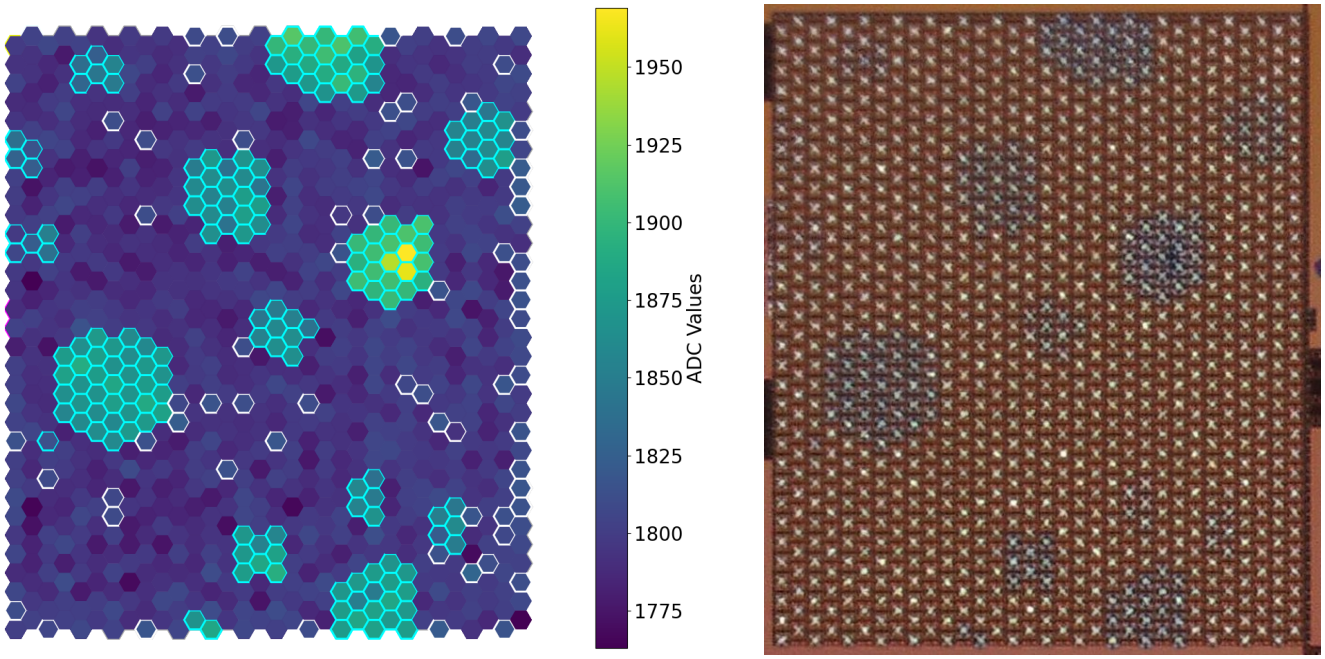

(a) Machine learning prediction

(b) Image by high resolution microscope

Figure D.1: Ink prediction of the cyan inked chip.

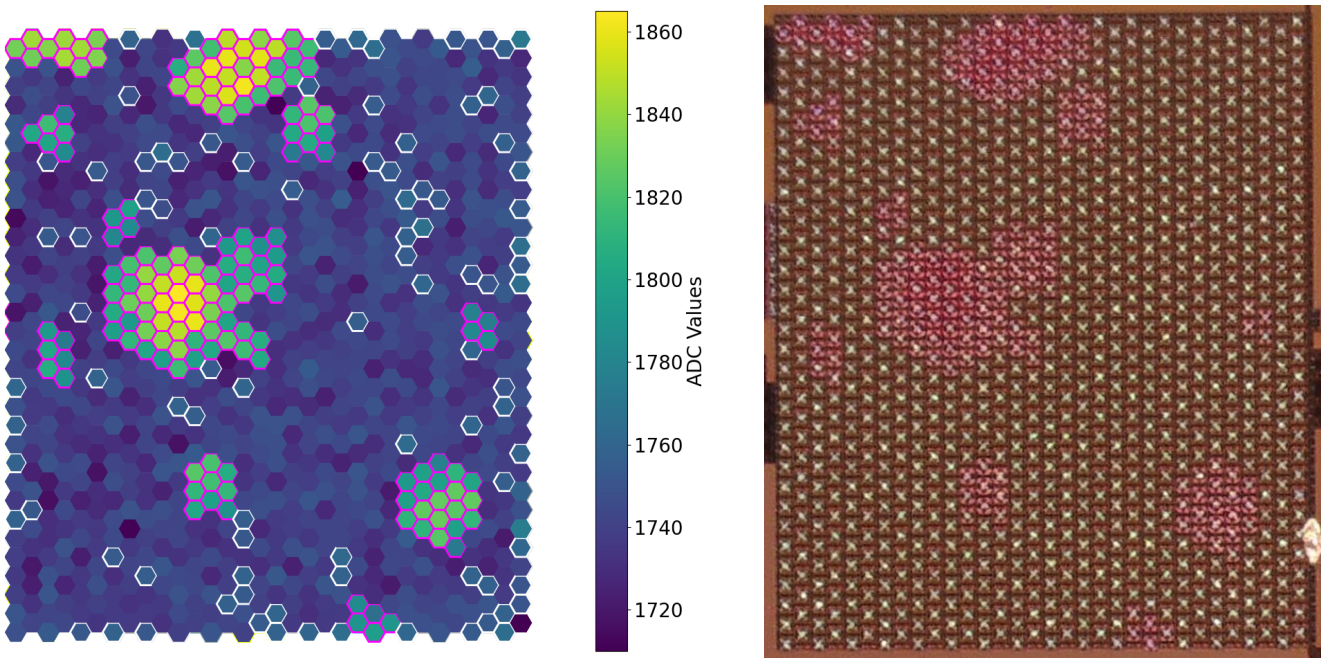

(a) Machine learning prediction

(b) Image by high resolution microscope

Figure D.2: Ink prediction of the magenta inked chip.

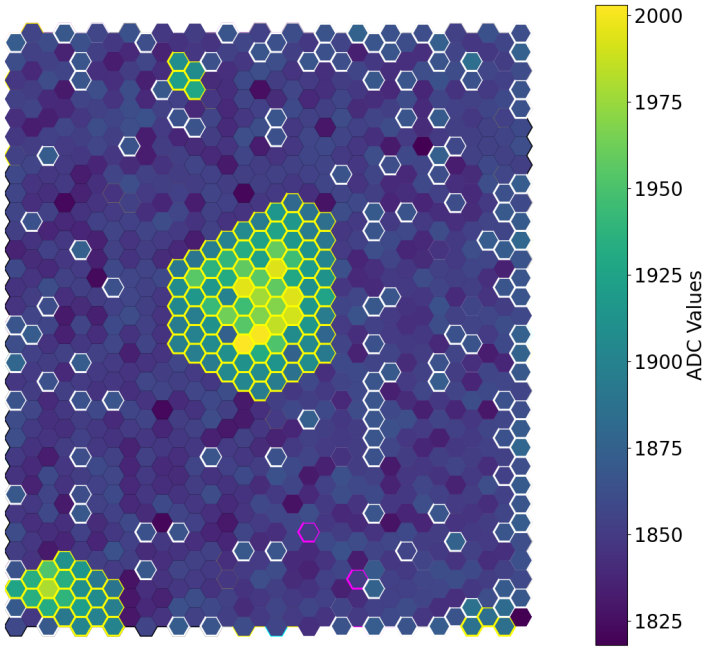

(a) Machine learning prediction

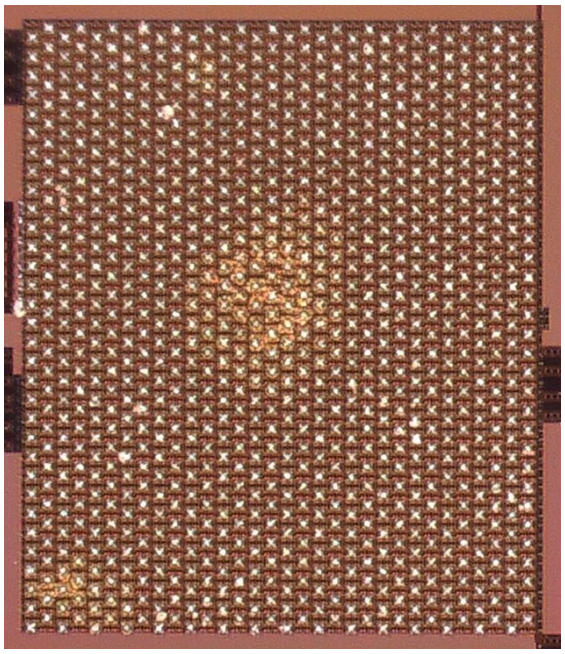

(b) Image by high resolution microscope

Figure D.3: Ink prediction of the yellow inked chip.

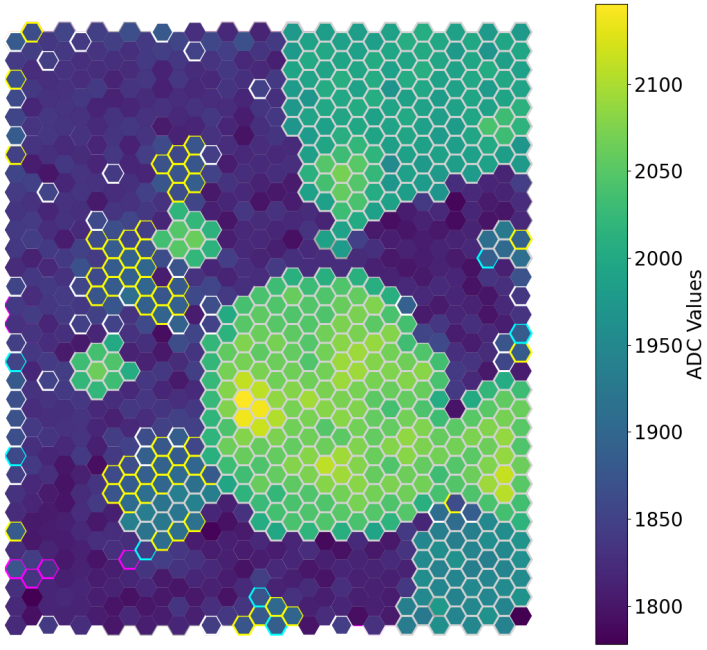

(a) Machine learning prediction

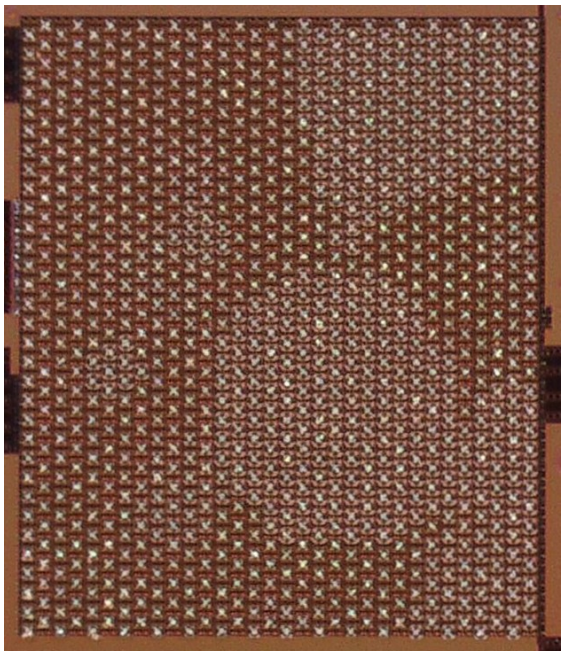

(b) Image by high resolution microscope

Figure D.4: Ink prediction of the grey inked chip.

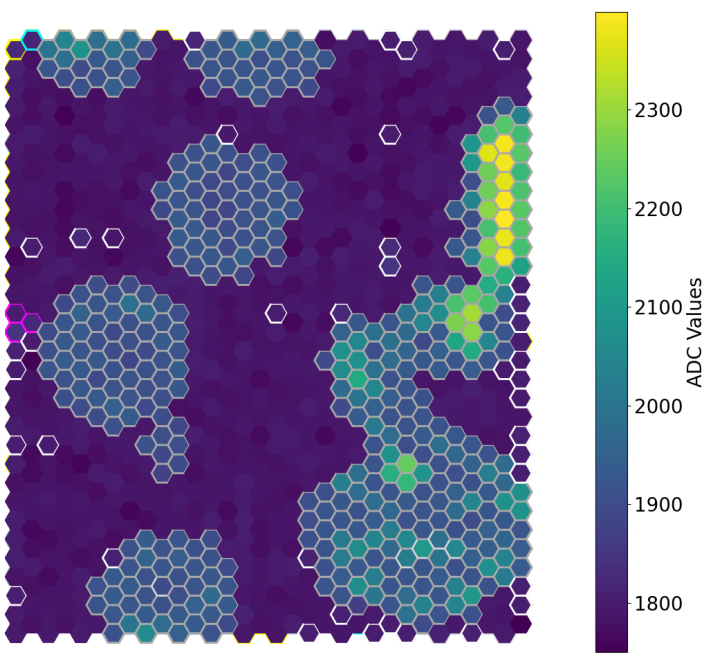

(a) Machine learning prediction

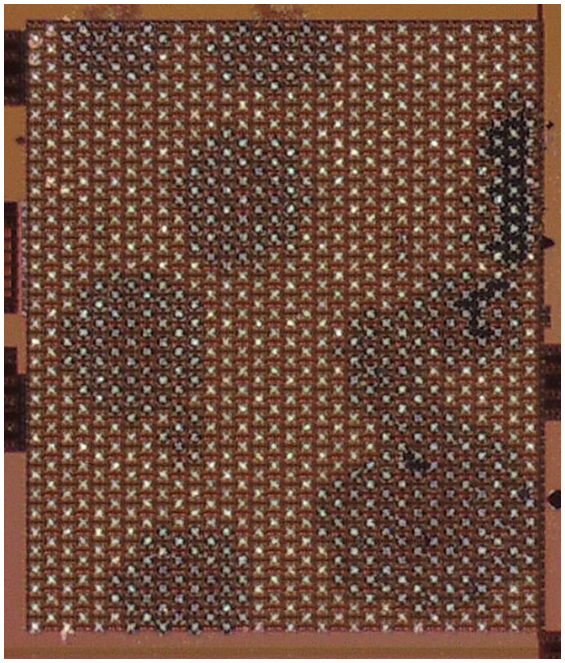

(b) Image by high resolution microscope

Figure D.5: Ink prediction of the black inked chip.

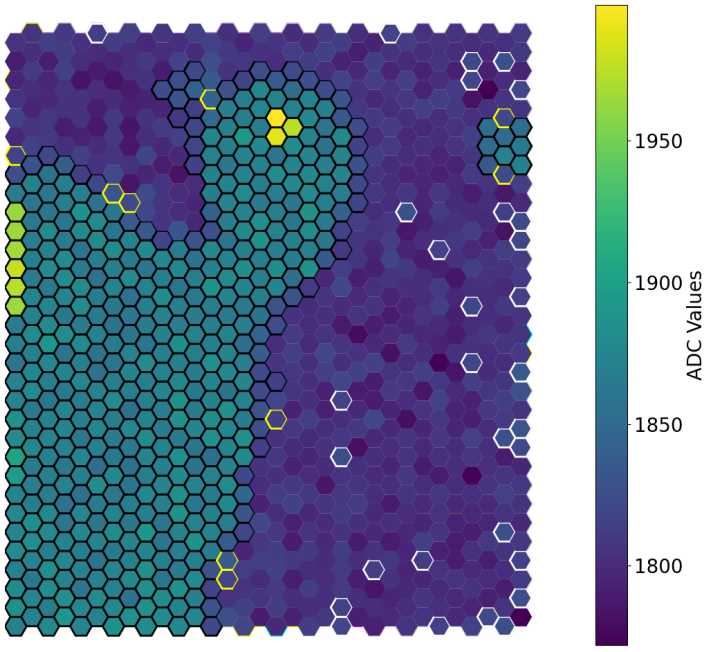

(a) Machine learning prediction

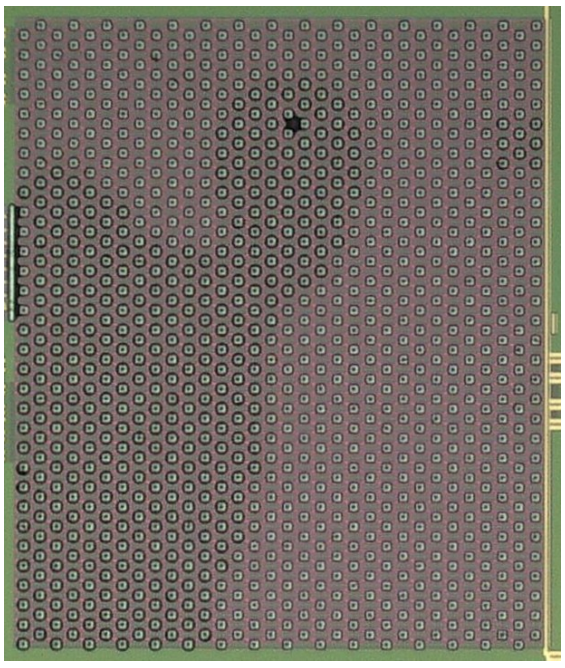

(b) Image by high resolution microscope

Figure D.6: Ink prediction of the photo-black inked chip. In order to see the photo black ink under the microscope, a side light setting needed to be used.

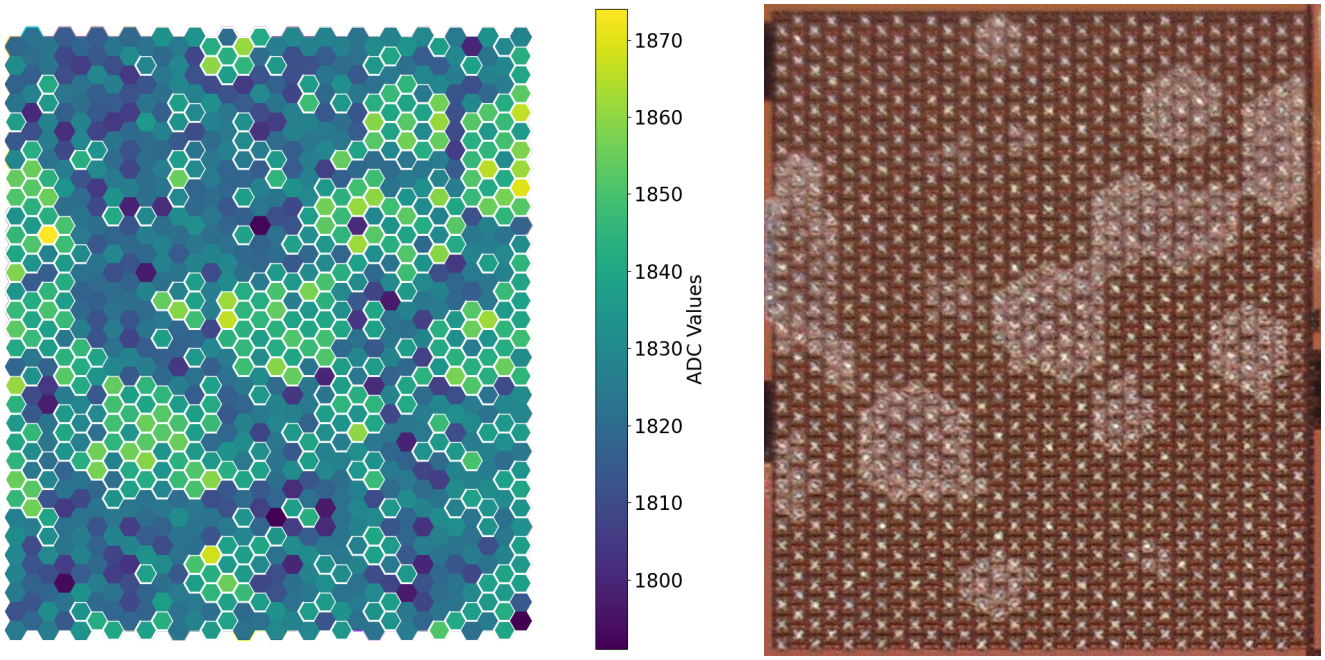

(a) Machine learning prediction

(b) Image by high resolution microscope

Figure D.7: Ink prediction of the white inked chip.

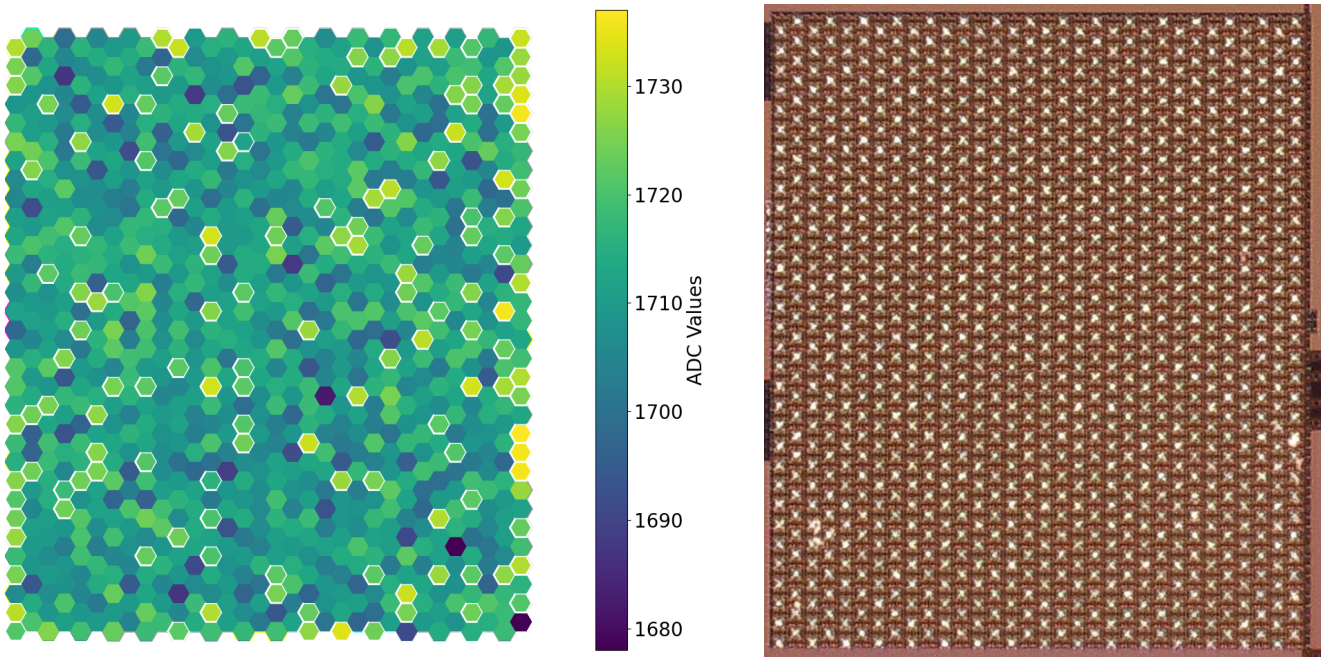

(a) Machine learning prediction

(b) Image by high resolution microscope

Figure D.8: Ink prediction of the empty chip.